TABLE 1
FOS OBSERVATIONAL PARAMETERS: M31 GLOBULAR CLUSTERS AND ELLIPTICAL GALAXIES

Name	R. A.	Dec	E(B-V)	$Mg_2$	$V_{\mathrm{H}}$	Data Set	Date of	Obs Time	` /	O
	(J2	2000)	mag	mag	${\rm km~s^{-1}}$	${ m ID}^1$	Obs	Exposure	Setup	Na
Globular Clusters										
K58	00:40:26	+41:27:26	0.080	0.213	-213	y17c01	21/01/93	2756	1485	V55
K280	00:44:29	+41:21:35	0.080	0.184	-164	y17c04	17/10/93	2794	705	V282,
MII	00:32:46	+39:34:39	0.080	0.148	-331	y17c52	19/11/93	2794	450	]
						y17c0206t	18/01/93	$0^3$	0	
MIV	00:43:17	+39:49:12	0.080	0.038	-270	y17c03	20/01/93	2794	825	K219,
Ellipitical Galaxies										
NGC 3605	11:16:46	+18:01:02	0.000	0.241	649	y39x01	06/06/96	10600	1408	UGO
NGC 3608	11:16:58	+18:08:55	0.000	0.329	1205	y39x02	06/12/96	10600	958	UGO
NGC 5018	13:13:01	-19:31:07	0.055	0.210	2794	y39x03	20/12/96	10600	1408	UGO
NGC 5831	15:04:07	+01:13:10	0.040	0.303	1924	y39x06	28/07/96	10600	1102	UGO
NGC 6127	16:19:11	+57:59:03	0.035	0.322	4609	y39x04	13/07/96	9030	1453	NGC 6128
NGC 7619	23:20:14	+08:12:21	0.000	0.358	3804	y39x05	13/07/96	3370	1408	UGC
						y39x55	22/11/96	10600	1408	

<sup>&</sup>lt;sup>1</sup>The data identification is in the form of instrument name (y=FOS), program ID (39x or17c), and observation set ID (eg. 55). fields (replaced with . . .) are individual exposures within that set of observations.

 $<sup>^2</sup>$ Names taken from SIMBAD. K = Sargent et al. 1977 numbers; Bol = Bologna numbers, taken from Battistini et al. 1980; 198  $^3$ observed with G130H grating on Blue detector — unusable due to geo-coronal L-alpha and OI 1300 emission

 ${\bf TABLE~2} \\ {\bf Definitions~for~Line~Indices~and~Colors}$ 

Feature Name	Blue P	assband	Index P	assband	Red Pa	ssband	Comments & Source
	(Å)	(Å)	(Å)	(Å)	(Å)	(Å)	
2000 2000	9470	0.670			2020	2120	2 EODW (1000)
2600–3000 F- II 2402	2470	2670	0200	0.400	2930	3130	3, FOBW (1990)
Fe II 2402	2285	2325	2382	2422	2432	2458	2, "
BL 2538	2432	2458	2520	2556	2562	2588	2, "
Mg Wide	2470	2670	2670	2870	2930	3130	2, "
Fe II 2609	2562	2588	2596	2622	2647	2673	2, "
2609/2660	2596	2623	• • •		2647	2673	3, "
Fe I+II + CrI	2647	2673	2736	2762	2762	2782	2, "
Mg II 2800	2762	2782	2784	2814	2818	2838	2, "
Mg I 2852	2818	2838	2839	2865	2906	2936	2, "
2828/2921	2818	2838			2906	2936	3, "
Fe I 3000	2906	2936	2965	3025	3031	3051	2, "
BL 3096	3031	3051	3086	3106	3115	3155	2, "
UV continuum	3150	3250			4180	4290	3, Davidge&Clark (1994)
NH 3360	3320	3350	3350	3400	3415	3435	1, "
Bl 3580	3500	3540	3540	3600	3620	3650	1, "
Balmer	3600	3700			4250	4290	3, "
4000	3750	3950			4050	4250	3, "
CN 3883	3760	3780	3780	3900	3900	3915	2, "
Ca HK	3900	3915	3915	4000	4000	4020	1, "
CN 4170	4082	4118	4144	4178	4246	4284	2, BFGK (1984)
$CH = G \ 4300$	4268	4283	4283	4317	4321	4336	1, "
Fe 4383	4360	4372	4370	4422	4444	4456	1, Worthey <i>et al.</i> (1994)
Ca 4455	4447	4455	4453	4476	4478	4493	1, "
Fe 4531	4506	4516	4516	4561	4562	4581	1, "
$C_2 \ 4668$	4613	4632	4635	4722	4744	4758	1, "
- 2				,			,

 $<sup>^11=</sup>$  Equivalent width (in Å); 2= magnitude; 3= band ratio or color (in mag)

TABLE 3A ULTRAVIOLET/VIOLET SPECTRAL INDICES AND COLORS - GLOBULAR CLUSTERS

Feature	$Type^1$	M:	32	K	58	K2	80	M	II	M	IV
	<i>J</i> 1	Obs	${\rm Err}^2$	Obs	$\operatorname{Err}$	Obs	$\operatorname{Err}$	Obs	$\operatorname{Err}$	Obs	$\operatorname{Err}$
2600-3000	3	1.496		1.509	0.047	1.003	0.013	0.689	0.008	0.373	0.014
Fe II 2402	$\frac{3}{2}$			1.453	0.554	0.182	0.066	0.287	0.039	0.244	0.064
BL 2538	2	0.483		0.735	0.302	0.331	0.063	0.348	0.038	0.212	0.060
Mg Wide	2	0.264		0.228	0.037	0.200	0.012	0.097	0.009	0.018	0.015
Fe II 2609	2	0.458		0.616	0.162	0.383	0.044	0.407	0.027	0.219	0.046
2609/2660	3	0.799		0.990	0.143	0.633	0.038	0.578	0.025	0.265	0.041
Fe I+II +C	$\overset{\circ}{2}$	0.357		0.444	0.142	0.247	0.046	0.188	0.031	0.074	0.050
Mg II 2800	2	0.737		1.127	0.160	0.693	0.044	0.650	0.028	0.368	0.046
Mg I 2852	2	0.358		0.583	0.105	0.401	0.035	0.320	0.024	0.069	0.040
2828/2921	3	0.534		0.608	0.085	0.490	0.030	0.327	0.021	0.061	0.037
Fe I 3000	2	0.177		0.195	0.061	0.156	0.024	0.122	0.018	0.012	0.033
BL 3096	2	0.100		0.252	0.072	0.206	0.028	0.146	0.022	0.063	0.041
UV continuum	3			1.141	0.025	1.126	0.009	0.877	0.008	0.680	0.016
NH 3360	1			7.879	2.973	8.253	1.062	7.560	0.912	3.687	2.052
Bl 3580	1			7.241	2.615	8.965	0.962	4.366	0.880	-0.429	1.960
Balmer	3			0.684	0.031	0.637	0.012	0.580	0.010	0.495	0.023
4000	3			0.616	0.018	0.643	0.007	0.456	0.006	0.202	0.012
CN 3883	2			0.286	0.055	0.333	0.020	0.200	0.017	0.061	0.035
Ca HK	1			22.915	3.117	23.927	1.111	19.807	1.051	9.935	2.564
CN 4170	2			0.132	0.040	0.054	0.015	-0.003	0.013	-0.082	0.029
CH = G 4300	1			6.687	1.304	4.682	0.525	2.252	0.540	0.393	1.261
Fe 4383	1			-1.512	2.604	4.503	0.836	2.203	0.822	0.500	1.947
Ca 4455	1			1.372	1.317	1.069	0.556	0.772	0.494	-0.500	1.208
Fe 4531	1			3.260	2.050	2.788	0.802	1.788	0.778	-0.534	1.981
$C_2 \ 4668$	1			4.583	3.061	3.256	1.163	1.289	1.140	-1.491	2.868
$C_2 \ 4668$	1	• • •	• • •	4.583	3.061	3.256	1.163	1.289	1.140	-1.491	2.868

 $<sup>^11=</sup>$  Equivalent width (in Å); 2 = magnitude; 3 = band ratio or color (in mag)  $^2\mathrm{One}\text{-sigma}$  errors. No errors are calculated for IUE data (M32).

TABLE 3BULTRAVIOLET/VIOLET SPECTRAL INDICES AND COLORS - ELLIPTICAL GALAXIES

Feature	$\mathrm{Type}^1$	N36	605	N36	808	N50	)18	N58	331	N61	127	N76	619
		Obs	$\mathrm{Err}^2$	Obs	Err								
2000 0000		1 051	0.000	1.010	0.010	1 000	0.110	0.005	0.001	1 200	0.005	0.700	0.000
2600–3000 F. H. 2402	3	1.371	0.032	1.018	0.018	1.326	0.113	0.807	0.021	1.266	0.067	0.739	0.023
Fe II 2402	2	0.108	0.173	0.096	0.087	-0.130	0.949	0.057	0.102	0.249	0.348	0.068	0.111
BL 2538	2	0.475	0.169	0.195	0.088	0.780	0.771	0.189	0.098	0.556	0.336	0.121	0.102
Mg Wide	2	0.282	0.027	0.235	0.018	0.355	0.097	0.180	0.022	0.230	0.058	0.181	0.025
Fe II 2609	2	0.392	0.113	0.318	0.063	0.165	0.392	0.203	0.074	0.270	0.223	0.142	0.080
2609/2660	3	0.612	0.097	0.496	0.056	0.473	0.344	0.355	0.066	0.468	0.200	0.298	0.073
Fe I $+$ II $+$ C	2	0.304	0.099	0.184	0.064	0.229	0.359	0.082	0.079	0.248	0.209	0.134	0.095
Mg II 2800	2	0.533	0.090	0.431	0.060	0.611	0.334	0.314	0.069	0.454	0.185	0.173	0.077
Mg I 2852	2	0.389	0.072	0.448	0.052	0.210	0.225	0.255	0.060	0.484	0.159	0.334	0.069
2828/2921	3	0.578	0.062	0.552	0.044	0.655	0.198	0.456	0.053	0.475	0.128	0.402	0.059
Fe I 3000	2	0.252	0.046	0.262	0.033	0.105	0.133	0.207	0.041	0.207	0.091	0.169	0.047
BL 3096	2	0.172	0.054	0.188	0.039	0.113	0.150	0.135	0.047	0.129	0.103	0.165	0.054
UV continuum	3	1.338	0.017	1.477	0.012	1.236	0.056	1.412	0.015	1.308	0.032	1.481	0.017
NH 3360	1	4.244	1.926	3.957	1.409	-2.688	5.696	3.040	1.738	2.352	3.570	5.260	1.886
Bl 3580	1	6.002	1.841	13.540	1.129	9.836	4.385	10.740	1.509	9.823	2.917	11.993	1.605
Balmer	3	0.697	0.021	0.775	0.014	0.750	0.054	0.833	0.018	0.753	0.035	0.807	0.019
4000	3	0.716	0.012	0.768	0.009	0.511	0.029	0.769	0.011	0.688	0.021	0.763	0.012
CN 3883	2	0.314	0.037	0.355	0.027	0.217	0.087	0.347	0.033	0.291	0.064	0.330	0.036
Ca HK	1	22.533	2.013	24.205	1.465	19.521	5.211	22.761	1.781	24.174	3.246	22.153	1.845
CN 4170	2	0.068	0.025	0.178	0.018	0.060	0.065	0.150	0.022	0.077	0.044	0.182	0.025
$CH = G \ 4300$	1	4.273	0.936	5.060	0.601	3.376	2.530	4.439	0.772	5.696	1.471	5.197	0.819
Fe 4383	1	5.178	1.311	3.985	0.940	2.136	3.720	4.944	1.111	5.361	2.343	4.325	1.243
Ca 4455	1	2.357	0.751	1.822	0.524	1.351	2.177	3.340	0.587	2.955	1.211	1.369	0.727
Fe 4531	1	3.850	1.247	3.320	0.850	3.248	3.369	4.516	0.979	5.492	0.018	3.869	1.112
$C_2 \ 4668$	1	9.645	1.763	7.232	1.302			9.313	1.691				

 $<sup>^11=</sup>$  Equivalent width (in Å); 2 = magnitude; 3 = band ratio or color (in mag)  $^2{\rm One\textsc{-}sigma}$  errors.

TABLE 4 GALACTIC GLOBULAR CLUSTER DATA

NGC Number	$\begin{array}{c} 2600 – 3000^{1} \\ \text{mag} \end{array}$	Mg I 2852 <sup>1</sup> mag	Mg II 2800 <sup>1</sup> mag	$\frac{2609/2660^{1}}{\text{mag}}$	2828/2921 <sup>1</sup> mag	${ m Mg_2}^2$ mag	$[\mathrm{Fe/H}]^3$
NGC 104	1.350	0.450	1.060	0.880	0.550		-0.76
NGC 362	0.740	0.200	0.670	0.530	0.290		-1.16
NGC 1904	0.400	0.110	0.450	0.290	0.120		-1.54
NGC 2808	0.600	0.110 $0.150$	0.670	0.650	0.310		-1.37
NGC 5139	0.500	0.120	0.510	0.370	0.100		-1.62
NGC 5272	0.850	0.100	0.700	0.480	0.190	0.042	-1.57
NGC 5904	0.590	0.210	0.500	0.470	0.280	0.064	-1.29
NGC 6093	0.390	0.100	0.450	0.290	0.160		-1.62
NGC 6205	0.450	0.130	0.440	0.310	0.130	0.043	-1.54
NGC 6266	0.510	0.220	0.540	0.420	0.240		-1.29
NGC 6284	0.400	0.120	0.540	0.280	0.160		-1.32
NGC 6293	0.460	0.140	0.350	0.270	0.130		-1.92
NGC 6341	0.400	0.110	0.290	0.170	0.100	0.013	-2.29
NGC 6388	1.100	0.230	0.730	0.820	0.490		-0.60
NGC 6441	1.390	0.410	0.830	1.420	0.720		-0.53
NGC 6624	0.940	0.450	0.960	0.480	0.600	0.154	-0.42
NGC 6637	1.150	0.260	0.980	0.820	0.500	0.134	-0.71
NGC 6681	0.460	0.180	0.490	0.270	0.160		-1.51
NGC 6715	0.600	0.200	0.560	0.440	0.170		-1.59
NGC 6752	0.420	0.110	0.550	0.330	0.200		-1.55
NGC 6864	0.890	0.290	0.620	0.580	0.110		-1.32
NGC 7078	0.470	0.120	0.330	0.230	0.120	0.017	-2.22
NGC 7089	0.450	0.160	0.490	0.320	0.120 $0.120$	0.052	-1.62
NGC 7099	0.310	0.090	0.320	0.200	0.020		-2.12
1.30 1000	0.010	0.000	0.020	0.200	0.020		

 $<sup>^1\</sup>mathrm{Line}$  strengths and spectral breaks from Rose & Deng (1998), as measured from IUE LWP data. No poisson errors are calculable for the IUE data.

<sup>2</sup>Optical Mg<sub>2</sub> taken from BFGK (1984).

<sup>3</sup>[Fe/H] values taken from WEB page of Harris (1997)

 ${\rm TABLE~5a}$  2600-3000 Colors for Davidge and Clark Stars

HD	2600-3000 mag	$\mathrm{Src}^1$	Sp Typ <sup>2</sup>
72324	2.58	1	G9 III
75732	2.31	1	G8 V
90277	0.73	2	F0 V
102634	1.35	2	F7 V
111631	2.90	2	M0.5 V
114710	1.56	1	G0 V
139669	2.35	2	K5~III
146051	1.73	2	M0~III
148856	2.39	2	G7 III
149661	2.01	2	K2 V
154633	1.82	2	G5 V
154733	2.35	2	K4 III
156653	0.08	2	A1 V
187642	0.40	2	A7 V

 $^{1}$ Source of 2600–3000 color: 1 = from Fanelli et al. (1990) direct observation; 2 = inferred from stellar groups as determined by Fanelli et al. (1992).

 $<sup>^2</sup>$ Spectral Types as listed by Davidge & Clark (1994).

TABLE 5BLICK CN4170, 2600-3000 Measures for Stars

4614       GO V       1.31       -0.073       6203       K0 III       3.00       0         10307       G2 V       1.56       -0.061       10380       K3 III       2.98       0         10476       K1 V       2.12       -0.018       10700       G8 V       1.74       -0	0.071 0.150 0.208 0.059 0.073 0.114 0.034 0.075 0.027 0.287 0.324
4614       GO V       1.31       -0.073       6203       K0 III       3.00       0         10307       G2 V       1.56       -0.061       10380       K3 III       2.98       0         10476       K1 V       2.12       -0.018       10700       G8 V       1.74       -0	0.150 0.208 0.059 0.073 0.114 0.034 0.075 0.027 0.287
10307 G2 V 1.56 -0.061 10380 K3 III 2.98 10476 K1 V 2.12 -0.018 10700 G8 V 1.74	0.208 0.059 0.073 0.114 0.034 0.075 0.027 0.287
10476 K1 V 2.12 -0.018 10700 G8 V 1.74 -	0.059 0.073 0.114 0.034 0.075 0.027 0.287
	0.073 0.114 0.034 0.075 0.027 0.287
10780 K0 V 2.15 -0.050   13043 G2 V 1.84 -	0.114 0.034 0.075 0.027 0.287
	0.034 0.075 0.027 0.287
	0.075 $0.027$ $0.287$
	$0.027 \\ 0.287$
	0.287
	() マワル
	0.075
	0.035
	0.165
	0.259
	0.112
	0.388
	0.286
	0.040
	0.074
	0.044
	0.294
	0.119
	0.352
	0.117
	0.088
	0.009
	0.011
	0.080
	0.006
	0.079
199629 A0 V 0.01 -0.063   200580 F9 V 1.21	0.063
	0.078
	0.043
215648 F6 III 1.34 -0.083 216385 F7 IV 1.31 -	0.126
217877 F8 V 1.69 -0.091 219134 K3 V 2.31	0.062
222368 F7 V 1.45 -0.080   224930 G2 V 1.52 -0.080	0.085

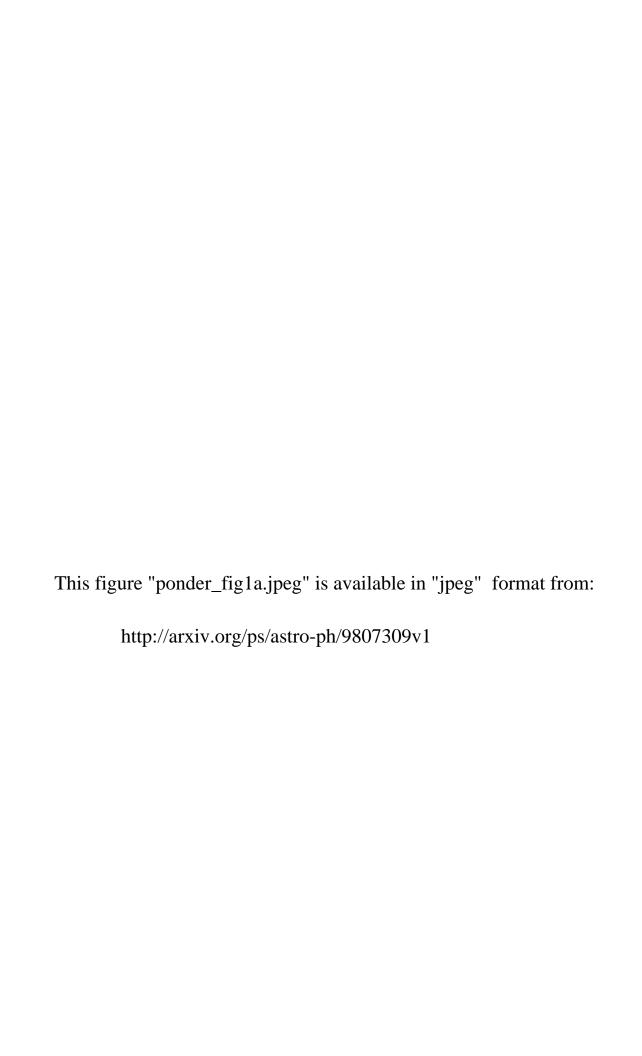
 $<sup>^1\</sup>mathrm{Spectral}$  Types as listed by Fanelli et al. (1990)  $^2\mathrm{IUE}$  2600–3000 colors taken from Li et al. (1998).  $^3\mathrm{CN4170}$  on original Lick system, from Worthey et al. (1994).

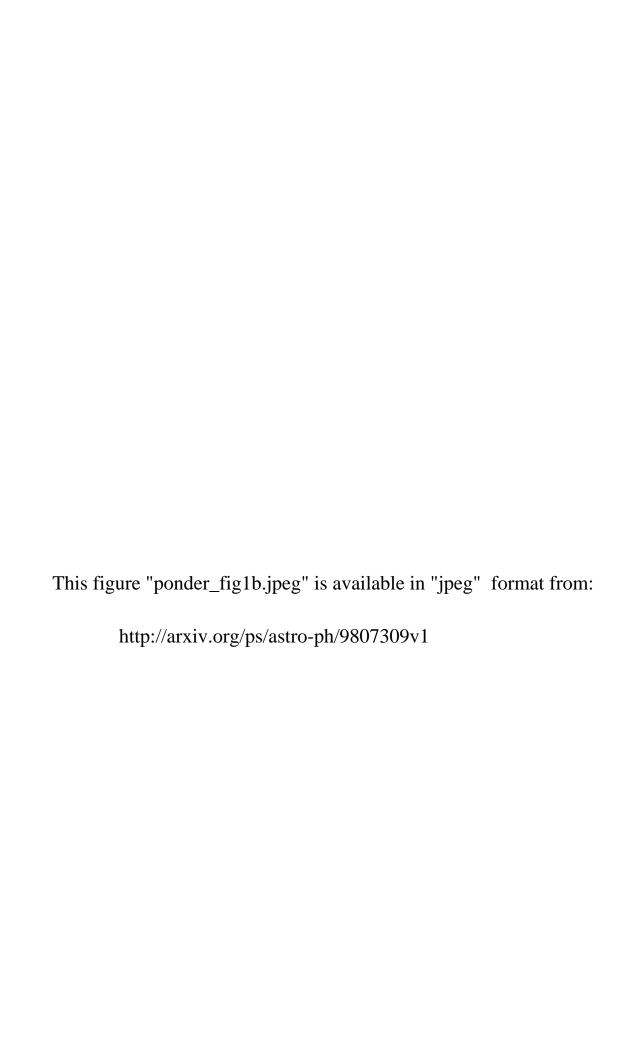
 $\begin{array}{c} {\rm TABLE~5c} \\ {\rm Elliptical~Galaxy~MG_2,~IUE~2600\text{--}3000~Colors} \end{array}$ 

NGC Number	${\rm Mg_2}^1$ ${\rm mag}$	$\begin{array}{c} 2600  3000^2 \\ \text{mag} \end{array}$
M 31	0.332	1.199
N 4382	0.332 $0.234$	1.189
N 4472	0.342	1.353
N 4552	0.351	0.839
N 4621	0.351	1.150
N 4649	0.373	0.835
N 5102	0.046	0.345

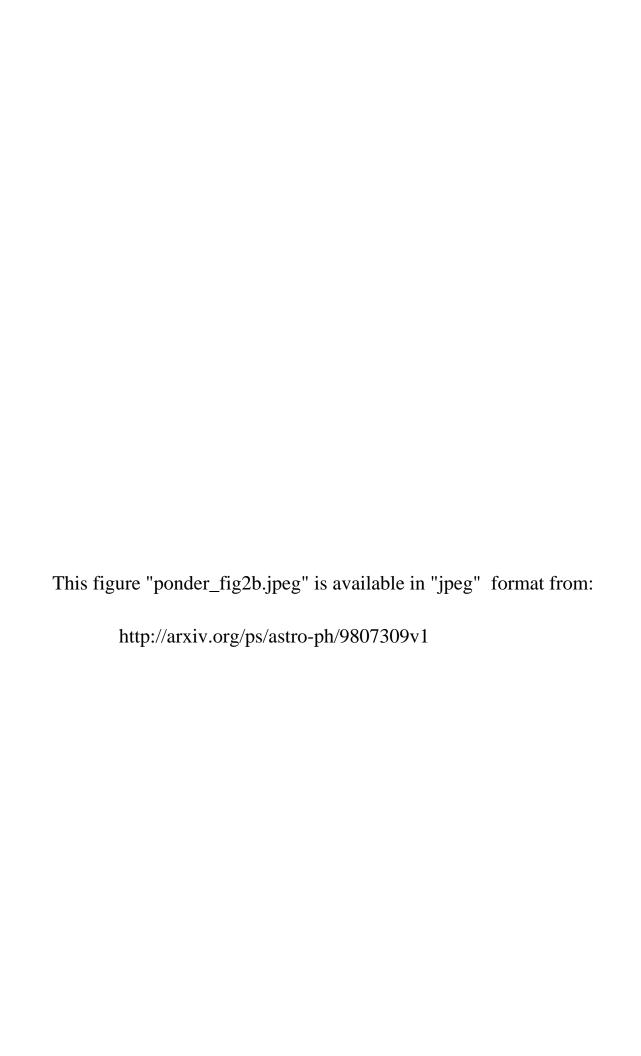
 $<sup>^{1}\</sup>mathrm{Mg_{2}}$  measures taken from Trager et al. (1998)

 $<sup>^{2}</sup>$ IUE 2600–3000 colors taken from Burstein et al. (1988).



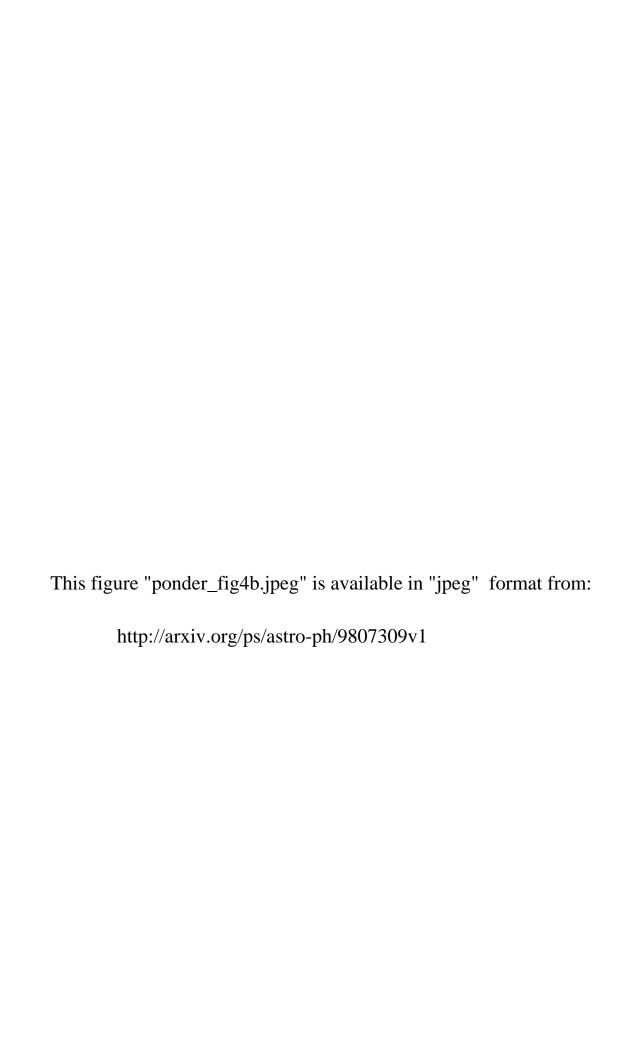


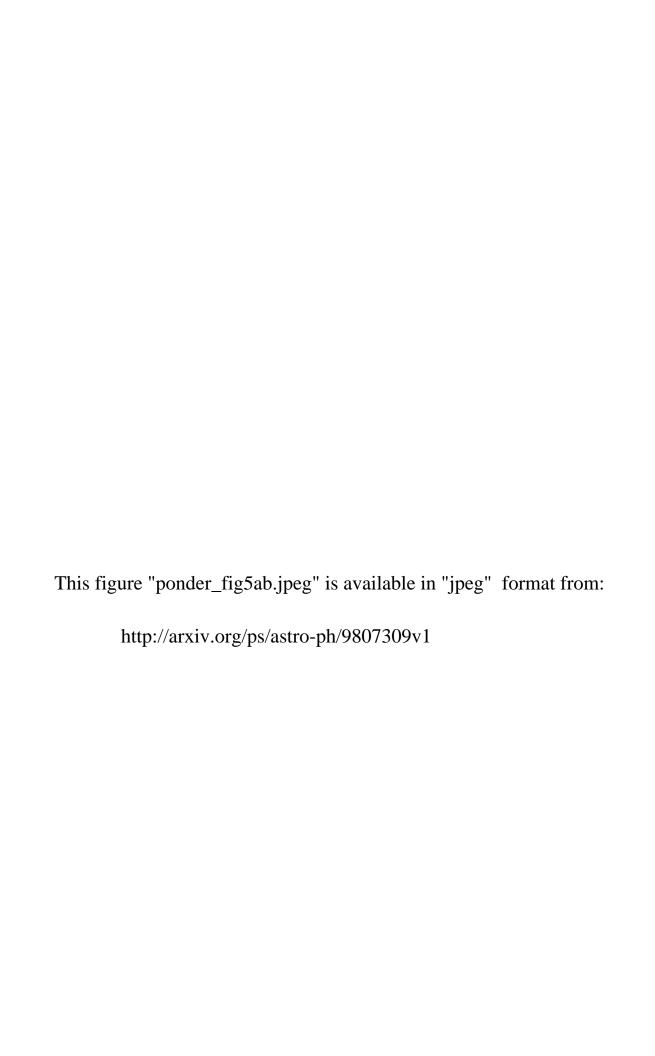










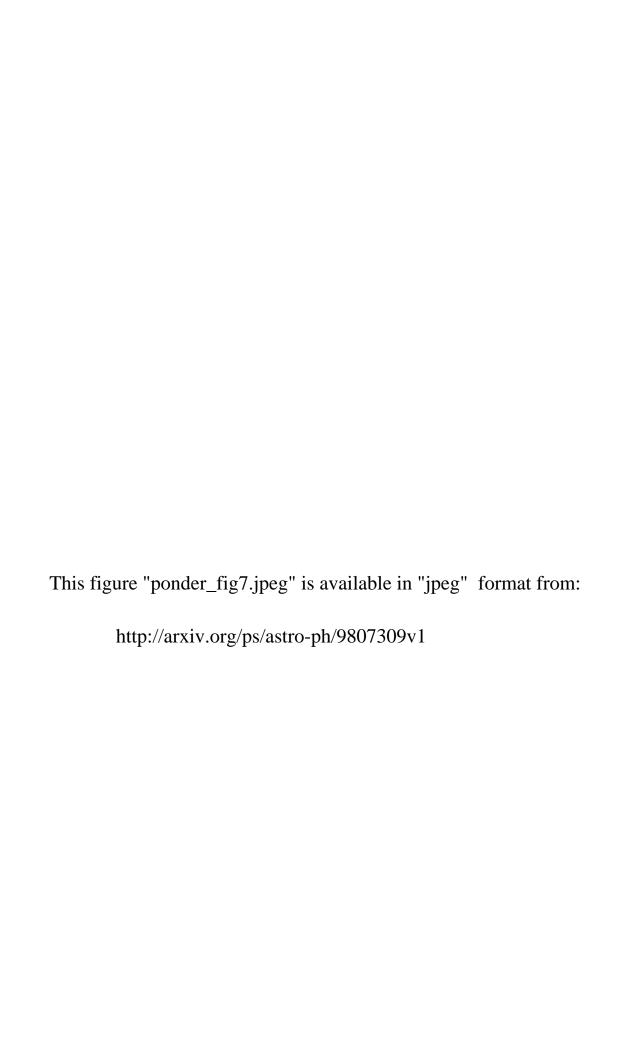


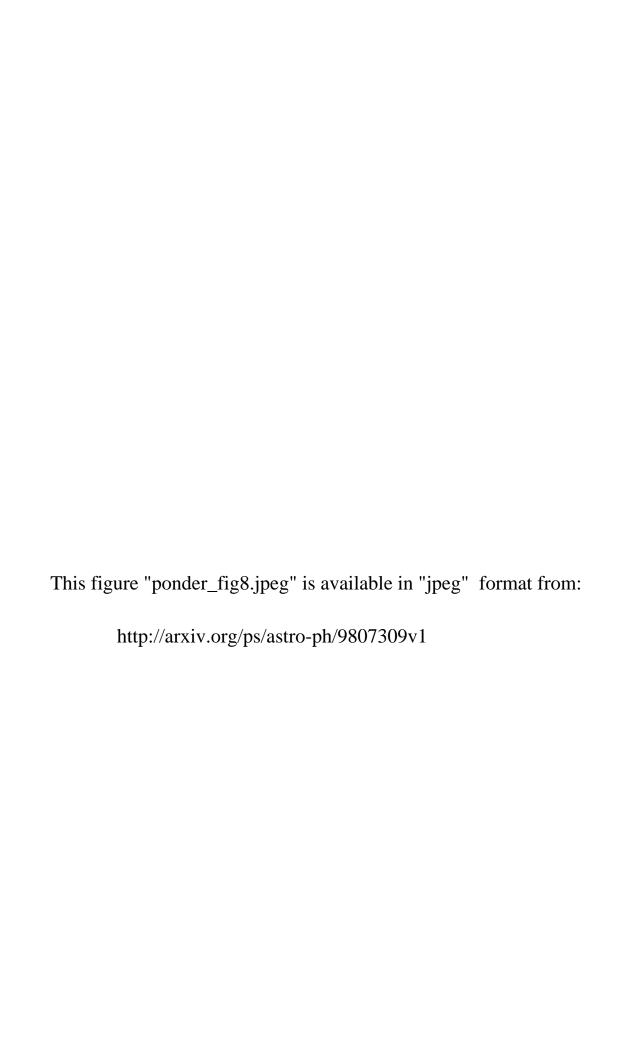


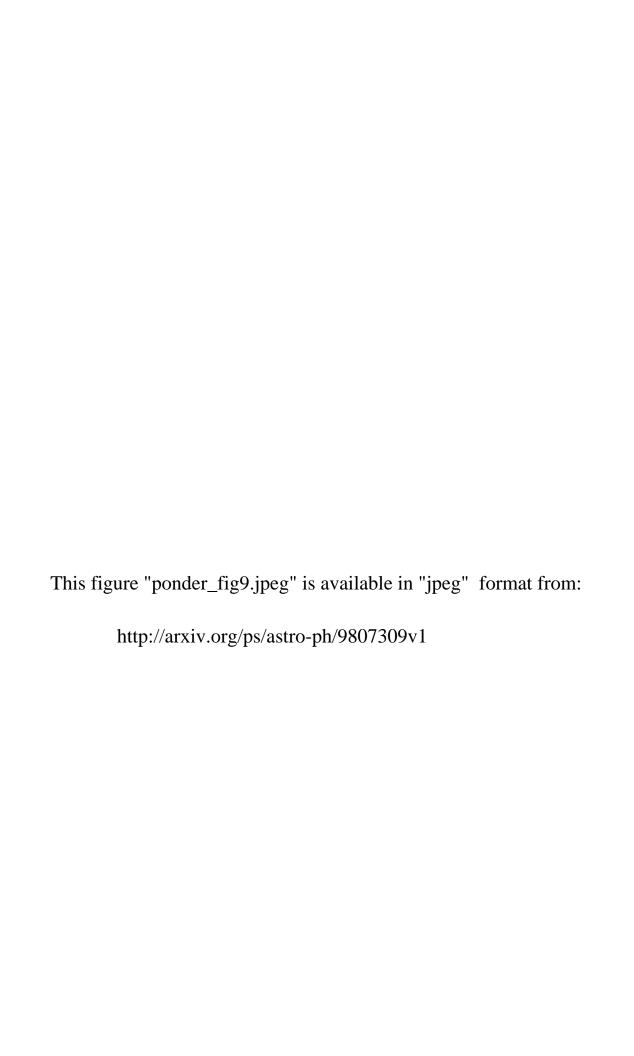


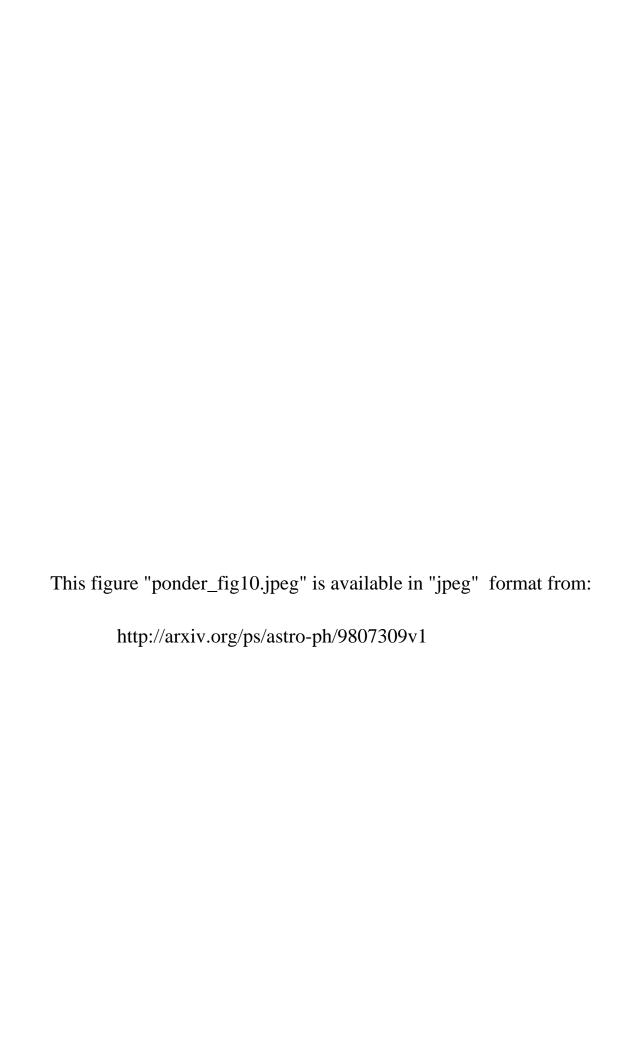












# Integrated UV Spectra and Line Indices of M31 Globular Clusters and the Cores of Elliptical Galaxies<sup>1,2</sup>

Jerry M. Ponder<sup>3</sup>, David Burstein<sup>3</sup>,

Robert W. O'Connell<sup>4</sup>,

James A. Rose<sup>5</sup>,

Jay A. Frogel<sup>6</sup>, Chi–Chao Wu<sup>7</sup>,

D. Michael Crenshaw<sup>8</sup>,

Marcia J. Rieke<sup>9</sup>, and Michael Tripicco<sup>10</sup>

# **ABSTRACT**

We present observations of the integrated light of four M31 globular clusters (MIV, MII, K280, and K58) and of the cores of six elliptical galaxies (NGC 3605, 3608, 5018, 5831, 6127, 7619) made with the Faint Object Spectrograph (FOS) on HST. The spectra cover the range 2200Å to 4800Å at a resolution

<sup>&</sup>lt;sup>1</sup>Based on observations with the NASA/ESA Hubble Space Telescope, obtained at the Space Telescope Science Institute, which is operated by the Association of Universities for Research in Astronomy, Inc., under NASA contract NAS 5-26555.

<sup>&</sup>lt;sup>2</sup>Based partly on observations obtained with the *International Ultraviolet Explorer Satellite*, which was sponsored and operated by the United States National Aeronautics and Space Administration, by the Science Research Council of the United Kingdom, and by the European Space Agency.

<sup>&</sup>lt;sup>3</sup>Department of Physics and Astronomy, Arizona State University. Box 871504, Tempe, AZ 85728-1504

<sup>&</sup>lt;sup>4</sup>Astronomy Department, University of Virginia, P.O. Box 3818, Charlotteville, VA 22903-0818

 $<sup>^5\</sup>mathrm{Department}$  of Physics and Astronomy, University of North Carolina, CB 3255, Phillips Hall, Chapel Hill, NC 27599-3255

 $<sup>^6</sup>$ Department of Astronomy, The Ohio State University, 174 W. 18th Ave, Columbus, OH 43210

<sup>&</sup>lt;sup>7</sup>Science Programs, Computer Sciences Corporation, Space Telescope Science Institute, 3700 San Martin Dr., Baltimore, MD 21218

<sup>&</sup>lt;sup>8</sup>Catholic University of America, Department of Physics, Washington, D.C. 20064

<sup>&</sup>lt;sup>9</sup>Steward Observatory, University of Arizona, Tucson, AZ 85721

<sup>&</sup>lt;sup>10</sup>NASA/Goddard Space Flight Center, Code 664, Greenbelt, MD 20771

of 8Å with S/N ratio > 20 and flux accuracy of  $\sim$  5%. To these data we add from the literature IUE observations of the dwarf elliptical M32, Galactic globular clusters and Galactic stars. The stellar populations in these systems are analyzed with the aid of mid–UV and near–UV colors and absorption line strengths. Included in the measured indices is the key NH feature at 3360Å. We compare these line index measures to the 2600–3000 colors of these stars and stellar populations.

We find that the M31 globular clusters, Galactic globular clusters/Galactic stars, and elliptical galaxies represent three distinct stellar populations, based on their behavior in color-line strength correlations involving Mg II, NH, CN, and several UV metallic blends. In particular, the M31 globular cluster MIV, as metal-poor as the Galactic globular M92, shows a strong NH 3360 feature. Other line indices, including the 3096Å blend that is dominated by lines of Mg I and Al I, show intrinsic differences as well. We also find that the broad-band line indices often employed to measure stellar population differences in faint objects, such as the 4000Å and the Mg 2800 breaks, are disappointingly insensitive to these stellar population differences.

We find that the hot  $(T>20000\mathrm{K})$  stellar component responsible for the "UV-upturn" at shorter wavelengths can have an important influence on the mid-UV spectral range (2400-3200~Å) as well. The hot component can contribute over 50% of the flux at 2600 Å in some cases and affects both continuum colors and line strengths. Mid-UV spectra of galaxies must be corrected for this effect before they can be used as age and abundance diagnostics.

Of the three stellar populations studied here, M31 globular clusters and elliptical galaxies are more similar to each other than each is to the Galactic stellar populations defined by globular clusters and nearby stars. Similarities between the abundance pattern differences currently identified among these stellar populations and those among globular cluster stars (N,Al enhancements) present a curious coincidence that deserves future investigation.

Subject headings: ultraviolet: galaxies — ultraviolet: M31 globular clusters — galaxies: elliptical and lenticular — galaxies: stellar content — globular clusters: stellar content

# 1. Introduction

The integrated spectra of galaxies are notoriously difficult to interpret in terms of their overall metallicity and age (cf. the excellent review by Charlot, et al. 1996). Every part of the spectral energy distribution (SED) of a stellar system yields a different clue to a complex puzzle. In the space-ultraviolet part of these SEDs we can unambiguously study the contribution of the hottest stars in stellar populations. The far-UV ( $\lambda\lambda 1250-2000\text{Å}$ ) and mid-UV ( $\lambda\lambda 2000-3300\text{Å}$ ) can most easily be studied in galaxies at high–redshift. Certainly, a prerequisite towards understanding the UV SEDs of galaxies at high redshift is to understand what we see in the UV SEDs of nearby stellar systems.

Towards the goal of understanding the UV SEDs of stellar populations, several of us have used the International Ultraviolet Explorer (IUE) to assemble a medium resolution (6Å) far-UV and mid-UV library of the spectral energy distributions of stars (Fanelli, et al. 1990; hereafter FOBW; Fanelli, et al. 1992; Li et al. 1998). In Fanellli et al. (1990, 1992) we found that the mid-UV color and absorption line indices have dependences on temperature and metallicity which are strong and distinct from those derived from spectra longward of 3300Å. In particular, Fanelli et al. (1992) found that absorption line measures using the usual index method (cf. O'Connell 1973; Faber 1973) yield mid-UV indices which are primarily sensitive to stellar temperature but insensitive to metallicity. One index in particular (MgII at 2800Å) is found to be inversely metallicity-sensitive for F–G dwarf stars, in that it gets weaker with increasing metallicity (cf. FOBW; Smith et al. 1991). In contrast, the mid-UV colors, which measure mean line blanketing, are found to the most sensitive to metallicity differences among stellar populations (FOBW).

Several groups have studied the far-UV and mid-UV SEDs of early-type galaxies and spiral galaxy bulges (e.g., Burstein, et al. 1988; Brown, et al. 1995), as well as of M31 globular clusters (e.g. Cacciari, et al. 1982; Cowley & Burstein 1988; Crotts, et al. 1990). From these studies we have learned that early-type galaxies contain a hot stellar population (T > 20000 K) whose amplitude, relative to the optical, is well correlated with stellar population absorption line strengths. Various studies indicate that this hot stellar population is important in galaxy spectra below  $\sim 3200 \text{Å}$ ; consists mainly of hot, metal rich, extreme horizontal branch stars and their post-HB descendents; and is very sensitive to the age and abundance of their parent population (e.g. Greggio & Renzini 1990, Brown, et al. 1995, Dorman et al. 1995, Tantalo, et al. (1996), and Yi et al. 1997).

The integrated light of Galactic globular clusters can usually be interpreted in terms of combinations of spectra of well understood field star populations near the Sun (cf. Christensen 1972; Rose 1994; Rose & Deng 1998). However, integrated optical line indices of M31 globular clusters exhibit anomalies which seem to distinguish them both from local field stars and Galactic globular clusters (cf. van den Bergh 1969; Burstein, et al. 1984;

Tripicco 1989; Brodie & Huchra 1990), especially concerning CNO-related indices (such as CN).

In the present paper we report on Hubble Space Telescope/Faint Object Spectrograph (HST/FOS) observations with small (< 1'') apertures of the 2300 - 4800Å SEDs of four M31 globular clusters and six bright elliptical galaxies. The galaxies chosen have old stellar populations that span the range known from optical observations (cf. Faber, et al. 1989, Gonzalez 1993). The M31 globular clusters were chosen to span a range of CN line strengths; all four have had their color-magnitude diagrams determined by HST imaging (cf. Fusi-Pecci et al. 1996). We combine these data with IUE-obtained mid-UV spectra of Galactic globular clusters and the dwarf elliptical galaxy M32. In §2 we discuss the FOS observations and present the observed spectra. In §3 we present a summary of the Galactic globular clusters and the M32 IUE data, which are detailed elsewhere. §4 details how the relationship between mid-UV line indices and the 2600-3000 color compare for the galaxies. M31 globular clusters, IUE data for Galactic stars and IUE data for Galactic globular clusters. §5 makes the analogous comparisons for the near–UV line indices. The various differences and similarities seen among the line stength-color relations for these stellar populations are discussed in §6. The main results of this paper are summarized in §7, and an Appendix discusses how the HST/FOS acquired each object for its science aperture.

## 2. Observations and Reductions

#### 2.1. Target Selection

Of the four M31 globular clusters chosen for study here, three (MII = K1, MIV = K219, and K280) had been previously studied in integrated light by Burstein et al. (1984) while a fourth (K58) comes from the integrated light study of Brodie & Huchra (1990). [The "K" names of the globular clusters are taken from the listing of Sargent, et al. (1977); "M" names from Mayall & Eggen (1953); "Bol" names from Battistini et al. 1980 and Battistini et al. 1987.] These globular clusters span the range from the most metal-poor (MIV) to the most metal-rich (K58) M31 clusters known.

The six galaxies were chosen to span a wide range of known stellar populations among old stellar systems as inferred by Gonzalez (1993). Gonzalez bases his estimates of galaxy ages on analyzing the strengths of H $\beta$ , mean Fe indices and the optical Mg<sub>2</sub> index with the galaxy population models of Worthey (1992). (Here, we explicitly state "the optical

Mg<sub>2</sub> index," so as to distinguish from the UV-based Mg-indices.) In his reanalysis of these data using the more up-to-date models of Charlot et al. (1996), Trager (1996) finds the rank-ordering of galaxy ages to be the same as Gonzalez. We note that while both Gonzalez and Trager provide independent estimates of age and metalliticy for their galaxies, in our samples age and metallicity (at least, strong absorption lines) are correlated (stronger lines  $\propto$  older ages).

The galaxies (in order of decreasing optical  $Mg_2$  strength) are: NGC 7619 ( $Mg_2 = 0.358$ ), NGC 3608 (0.329), NGC 6127 (0.322), NGC 5831 (0.303), NGC 3605 (0.241), NGC 5018 (0.210) and M32 (0.198). NGC 5018 is added to this sample, although not specifically observed by Gonzalez, as it has UV/optical colors and optical line strengths similar to that of M32, yet has the luminosity of a giant elliptical (Bertola, et al. 1993). Of this sample, only M31 and M32 have far–UV SEDs available (both from IUE; Burstein, et al. 1988). On the scale defined by the Worthey models, ages for these objects range from above 12 Gyr at the oldest, to 3–5 Gyr at the youngest, or  $Mg_2 = 0.35$  at the strongest-lined and 0.20 at the weakest-lined. We also note that none of these objects is expected to have a significant stellar population component of age less than 1 Gyr (cf. Gonzalez 1993; Trager 1996).

#### 2.2. Observations

FOS observations for the globular clusters were originally scheduled under HST/GO program P2298 for Cycle 1, but were obtained in Cycles 1, 2 and 4. FOS observations for the galaxies were taken under HST/GO program P6585 in Cycle 6. Table 1 contains the log of observations, with the HST archival name for each spectrum given for easy reference. Also given in Table 1 are J2000 positions for the objects observed, as well as their optical Mg<sub>2</sub> values and the radial velocities we used for them. The Mg<sub>2</sub> measures come from Burstein et al. (1984) for MII, MIV and K280. The Mg<sub>2</sub> values for K58 is transformed from that listed by Brodie & Huchra (1990) (by applying a net offset of +0.026 mag to bring their measures in accord with those of Burstein et al.). The Mg<sub>2</sub> measures for the galaxies come from Trager et al. (1998). All Lick Mg<sub>2</sub> observations were observed with a 1.4" × 4" slit (cf. Trager et al. 1998), so sample the clusters and galaxies at angular resolutions comparable to the HST observations. The radial velocities for the M31 globular clusters come from Huchra, Brodie & Kent (1991), while those for the galaxies come from de Vaucouleurs et al. (1991).

Given the diffuse nature of the objects studied, the FOS aperture for each observation

had to be centered via the FOS ACQ/PEAK-UP procedure to obtain the required positional accuracy within the nominal 1" circular aperture (for Cycles 1 and 2, pre-COSTAR, which becomes 0.86" for Cycles 4 and 6, post-COSTAR). The manner and accuracy of target acquisition are detailed in Appendix A.

The M31 globular clusters were observed with three FOS gratings: G130H, G270H and G400H. The G130H grating was used, despite its limited wavelength coverage, as it was suggested by previous IUE observations (e.g. Cacciari, et al. 1982) that some of the M31 globular clusters might contain a substantial hot stellar population. Although we took long integrations with the G130H grating, no significant signal in the full 1300–1600Å bandpass was measured for any of the M31 clusters (see discussion below). Thus, we do not find any very hot stellar populations in these clusters that falls within our aperture (of diameter 2.9 pc at the distance of M31). Combination of the G270H plus G400H gratings give us continuous wavelength coverage from 2300Å to 4800Å, with essentially no observational overhead.

As the galaxy spectra were obtained after the M31 globular cluster spectra, we knew that we would not likely get any scientific information from the G130H grating in a reasonable number (i.e., < 20) of orbits, so it was decided to concentrate only on getting accurate spectra with the G270H and G400H gratings. It typically took 6 orbits to obtain the spectra we show here for the galaxies, including 3.5 orbits to do the ACQ/PK procedure. Obtaining accurate UV spectra of diffuse objects with HST/FOS was expensive in time.

#### 2.3. Data Reduction

Our data reduction procedures followed those recommended by the HST/FOS Data Products Guide (Baum 1993; hereafter DPG). The data sent to us were processed by Space Telescope Science Institute with the Routine Science Data Processing software, which produces files of fluxes, wavelengths, errors, data qualities as well as raw data. As a check, we ran the raw data through our local IRAF/STSDAS programs and found no differences between the HST-provided data and our re-reduced data.

Flux and wavelength files were combined as recommended by the DPG, including resampling and Hanning smoothing of the data. Since the observed spectral resolution is finer than the spectral resolution permitted by the nominal 1" aperture, the spectra were further smoothed by a boxcar window of sufficient size to produce spectral resolution of 5.5Å for the G270H grating and 8.8Å for the G400H grating. The G270H spectra of two

galaxies (NGC 6127, NGC 5018) are noisier than for the other objects in this sample. Examination of the error spectrum for NGC 6127 shows that the apparent "emission" line at the position of the Mg 2800 line is an artifact resulting from low signal-to-noise and a diode in the FOS that had just gone bad.

As stated previously, we only were able to obtain upper limits for the observations of the M31 globular clusters obtained with the FOS G130H grating. Integrating the flux observed with this grating from 1300 to 1600Å we obtain:  $9.3 \pm 19 \times 10^{-17}$  ergs s<sup>-1</sup> cm<sup>-2</sup> for MII,  $0.8 \pm 19 \times 10^{-17}$  ergs s<sup>-1</sup> cm<sup>-2</sup> for K58 and  $1.3 \pm 18 \times 10^{-17}$  ergs s<sup>-1</sup> cm<sup>-2</sup> for MIV. The FOS shutter did not open for the observation of K280, so we use this observation to give us the background rate.

All spectra are dereddened, using the values of E(B–V) given in Table 1 and the reddening law of Cardelli et al. (1989), updated by O'Donnell (1994) for the near-UV. E(B–V) values are taken from Burstein & Heiles (1984) for the galaxies and for M31 (assuming the clusters are reddened only by foreground Milky Way extinction). Spectra of all objects were then Doppler-shifted to their rest wavelengths using the radial velocities given in Table 1. The de-reddened fluxes are given at rest wavelengths, and will be made available for each object in our sample in ASCII format via various electronic means, including: anonymous ftp; electronic preprint, and, eventually, the Astronomical Data Center.

The resulting spectra are shown in linear flux units in Figures 1a and 1b for the globular clusters and in Figures 2a and 2b for the galaxies, at their rest wavelengths. Figures 3, 4a and 4b show the full HST/FOS spectra of the clusters and the galaxies (plus the IUE mid-UV spectrum of M32) in log flux units. Spectra from the G270H grating and the G400 grating are shown separately in parts a and b of Figures 1 and 2 for clarity. A test of the zero point accuracy of the relative fluxes obtained from the two spectra can be derived from the 70Å overlap in the region 3200 – 3270 Å. As shown in Figures 3 and 4, the relative fluxes agree within the nominal value of 5% we are led to expect by the FOS Handbook.

## 2.4. Line Indices

Our spectra cover a range of UV and optical wavelengths for which no single unified set of absorption line and continuum indices has yet been defined. Rather, our choice of indices and colors come from three separate studies: a) The range 2300 to 3100 Å has

the mid-UV indices defined by FOBW. b) The range 3100 to 3800 Å have several indices defined by Davidge & Clark (1994), including the very useful NH molecular band at 3360Å. c) The range 3800 to 4800 Å is covered by Lick Observatory photometric systems (Worthey, et al. 1994). A list of the definitions of the line strength indices measured for our spectra, and the source of each index, is given in Table 2.

To determine the index values, we use the definitions of spectral indices given by Gonzalez (1993):

$$I_{a} = \int_{\lambda_{c_{1}}}^{\lambda_{c_{2}}} \left(1 - \frac{S(\lambda)}{C(\lambda)}\right) d\lambda \tag{1}$$

$$I_{\rm m} = -2.5 \log_{10} \int_{\lambda_{\rm c_1}}^{\lambda_{\rm c_2}} \frac{S(\lambda)}{C(\lambda)} d\lambda$$
 (2)

where  $S(\lambda)$  represents the object flux at each wavelength within the central bandpass,  $C(\lambda)$  represents the pseudo-continuum flux for  $S(\lambda)$  within the central bandpass, and  $\lambda_{c_1}$ and  $\lambda_{c_2}$  are the limits of the central bandpass. All fluxes in this paper are computed per unit wavelength. Equivalent width indices computed from Equation 1 are measured in angstroms; indices computed from Equation 2 are measured in magnitudes. Equation 2 is essentially identical to the line index definition of FOBW, differing negligibly (<< 0.001 mag) in practice. The pseudo-continuum within the central bandpass is determined by linear interpolation between the red and blue pseudo-continuum sidebands defined for each absorption feature. The wavelength ranges of the red and blue sidebands and the central bandpasses for the absorption features measured in this paper are given in Table 2. The spectral break indices and the intermediate band color index 2600-3000 are defined as the ratio of the mean fluxes within the appropriate bands converted to magnitudes. To account for uncertainties in the radial velocities and in the wavelength scales used, each spectral line measurement was adjusted interactively. We adjusted the continuum and feature passband positions (typically by less than 2 pixels) by comparing them with their placement given in the papers that define these line indices. The spectral indices and colors for all observations are given in Tables 3a,b.

Errors were determined from the error spectra provided by the pipeline reduction process. These error spectra are computed by propagating the errors at each point with the assumption that the dominant noise in the raw data is photon noise. We then determine the mean error based on photon statistics  $(\delta S(\lambda))$  or  $\delta C(\lambda)$  for each bandpass and propagate those errors through the previous equations, with the results:

$$\frac{\delta I_{a}}{I_{a}} = \frac{(\lambda_{1} - \lambda_{2})}{C(\lambda)} \sqrt{\left[(\delta S(\lambda))^{2} + \left(\frac{\delta C(\lambda) \times S(\lambda)}{C(\lambda)}\right)^{2}\right]},$$
(3)

$$\delta I_{\text{mag}} = \frac{2.5}{\ln(10)} \sqrt{\left[\frac{\delta S(\lambda)}{S(\lambda)}\right]^2 + \left[\frac{\delta C(\lambda)}{C(\lambda)}\right]^2}, \text{ and}$$
 (4)

$$\delta \text{Break} = \frac{2.5}{\ln(10)} \sqrt{\left[\frac{\delta S(\lambda)}{S(\lambda)}\right]^2}.$$
 (5)

The errors for our measured indices are given in Table 3 in terms of either magnitudes (for broad features and breaks) or equivalent widths (in Å).

# 3. Supplemental IUE Data

To supplement the HST observations, we have also included IUE-obtained data for the galaxy M32 (from Buson, et al. 1990) and for 24 Galactic globular clusters. The IUE globular cluster data come from the study of Rose & Deng (1998). Rose and Deng surveyed the IUE database and identified 24 Galactic globular clusters which have been observed by IUE in their core regions, and which have good quality mid-UV IUE low-resolution spectra. In the case of M32, we have derived all of the mid-UV line indices and 2600–3000 color (listed in Table 3a) from the data of Buson et al. In the case of the Galactic globular clusters, Rose and Deng derived only four of the mid-UV line indices (Mg I, Mg II, the 2609/2660 and 2828/2921 line breaks) plus the 2600–3000 color. The data for M32 appear in a subset of the line strength-color relations we compare to those of stars, while the Galactic globular cluster data appear only when we intercompare the line strengths of galaxies, M31 globular clusters and Galactic globular clusters. The IUE observations of M31 globular clusters and galaxies.

Details of the data reduction of IUE data are given in Rose & Deng (1998). In summary, most of the Galactic clusters have only a single IUE observation, but for the ones with multiple observations, the coadded spectra were used. We list the 24 globular clusters in Table 4, together with their IUE-based line strength measures from Rose & Deng, estimates of [Fe/H] taken from Harris (1997), and  $Mg_2$  measurements taken from Burstein et al. (1984). As the IUE aperture of  $10'' \times 20''$  covers a fairly large region of the cores of

most clusters, we believe the spectra are representative of the integrated mid-UV light of these cores. All of the IUE spectra were individually corrected for interstellar extinction by Rose and Deng using the reddening curve of Cardelli et al. (1989), as modified by O'Donnell (1994), with E(B-V) values from Peterson (1993).

# 4. Stellar Populations in the Mid-UV

# 4.1. Choosing an Appropriate Mid-UV Color

If we are to correctly interpret the absorption line measurements in the mid-UV, it is important to compare these measurements to a UV measure of temperature. As shown in FOBW, the 2600–3000 color is a reasonable compromise, in that: a) it can be self-consistently defined for mid-UV spectra, as well as reliably measured; and b) it is sensitive to the stellar population mix in the mid-UV. Within that stellar population mix we cannot ignore the contribution of the hot component which dominates the far-UV in elliptical galaxies. As shown in Burstein et al. (1988), this "UVX" component can contribute substantial flux at wavelengths as long as 3200 Å in some cases. UVX effects are clearly present in our galaxy sample. They are seen, for instance, in the anticorrelation between the 2600–3000 colors and the optical Mg<sub>2</sub> indices for these galaxies (cf. the data in Table 1 with those in Table 3a).

Tables 3a,b give reliable 2600–3000 colors for our program objects. Similarly, the stellar library from IUE (FOBW) has directly measured values of 2600–3000. Of the two other stellar libraries used here, it is profitable to estimate 2600–3000 colors only for the line indices of Davidge & Clark (1994), as these are closest in wavelength to the mid-UV. We list the measurements for additional indices from the Lick system in Tables 3a,b for reference only. We display our results in the form of (logarithmic) index-index diagrams below.

There are two main issues to be addressed here. First, do the galaxies and the two globular cluster systems differ significantly from each other in any index comparisons? We will see that they do. Second, is it possible to synthesize the composite systems (clusters or galaxies) by suitable combinations of the Galactic stellar library objects? We do not attempt actual spectral synthesis modeling in this paper, so it is important to understand where potential combinations would appear in the diagrams. A given index formed from any combination of stars is the weighted sum of the indices of its components, where the

weight  $w_i$  for component i is  $0 \le w_i \le 1.0$  and  $\Sigma w_i = 1.0$ . However, the weights will change with wavelength. This means that unless the two indices involve a common normalizing wavelength, a combination formed from two components will not fall exactly on the straight line connecting them in a ratio-ratio diagram, and their relationship will be further distorted in the logarithmic index diagrams shown here.

As discussed above, most of the galaxies have significant UVX contamination at wavelengths below 3200Å but the M31 globular clusters do not. This means that separations between clusters and galaxies in the index-index diagrams could be the result of feature dilution or bluing caused by the UVX component (which has a smooth energy distribution similar to that of an early B-type star, with a 2600–3000 color of  $\sim -0.5$ ). However, such separations are not necessarily only the result of UVX contamination, and we will try to distinguish between these two cases. On the other hand, those diagnostic diagrams in which the galaxies and M31 clusters are superposed but separated from the locus of Galactic library stars are indicative of other explanations for the separation: e.g. differences in chemical abundances.

# 4.2. Elliptical Galaxies and Globular Clusters in The Mid-UV

For clarity, we compare the line indices and spectrum breaks determined in our FOS G270 spectra and in the IUE LW spectrum for M32 to those for IUE-observed stars in Figures 5a-g. At the end of this section we will compare these values with the IUE values for Galactic globular clusters. Those indices with center wavelengths below 2550Å were not used, as the IUE data are generally too noisy shortward of this wavelength. The data for galaxies are plotted as open symbols; those for the M31 globular clusters are plotted as closed symbols; the data for Galactic stars are plotted as small, subdued symbols. All error bars are smaller than the plotting symbol for the 2600–3000 color, save for NGC 5018, and are not shown. Errors in the line indices are explictly shown in Figures 5. Each of the possible comparisons among the galaxies, M31 globular clusters, Galactic globular clusters, and Galactic stellar libraries is of interest.

Figure 5a: 2609/2660 break. The M31 clusters follow the locus of Galactic library stars well, but the galaxies other than M32 fall systematically below, with 2609/2660 values at a given 2600-3000 color up to 0.4 mag smaller. This is probably a result of UVX contamination in the galaxies; the implied contribution of the hot component in the galaxies at 2660 Å is about 60% in the most extreme case (NGC 7619; cf. Burstein, et al. 1988).

Figure 5b: 2828/2921 break. The values for the M31 globular clusters and the galaxies agree well, and both lie at somewhat stronger index measures compared to the stellar library at the same color. The offsets from the Galactic library locus here cannot be explained by UVX contamination in the galaxies. The two weakest clusters (MII and MIV) have 2828/2921 values lower than those of any galaxy.

Figure 5c: Mg II 2800 index. This is the line index with the paradoxical behavior with metallicity: it gets weaker as metallicity increases. Moreover, it is double-valued with 2600-3000 color (as is the 2609/2600 break), peaking near 2600-3000=1.5 (owing to chromospheric emission becoming greater with later-type stars; cf. FOBW, Smith et al. 1991). Both galaxies and M31 globular clusters show well-defined relationships between line index and color. The M31 clusters agree well with the locus of Galactic library stars. However, the galaxies have indices which are systematically  $\sim 0.3$  mag smaller than the clusters and the stars. This could be another instance of UVX contamination; however, for at least 3 of the galaxies the Mg I 2852 index (see below) does not show a similar offset despite immediate proximity in wavelength. This argues against UVX contamination as the main cause of the Mg II offset in the galaxies.

Figure 5d: Mg I 2852 index. Despite involving the same element, lying only 50Å from Mg II, and sharing a continuum sideband with the Mg II index, in this Mg I index the M31 clusters and galaxies behave very differently than in Mg II. Indices for three of the clusters are significantly stronger than in the Galactic library stars, and three of the galaxies are coincident with these clusters. The other five objects fall close to the stellar locus.

Figure 5e: Fe I 3000 index. As we have shown previously (FOBW), the Fe I 3000 index shows little direct correlation with metallicity among Galactic stars, but does show a strong temperature dependence. Here, five of the galaxies and two of the clusters have indices significantly higher than the Galactic library locus and the remaining four objects. This is the only UV index in which the galaxies have conspicuously stronger index values than the M31 globular clusters (note that for most optical-band metallic features, gE nuclei have stronger indices than do globular clusters).

Figure 5f: Blend 3096 index. This index is a combination of Al I (at 3092.7 Å) and Fe I lines. It was found in FOBW to have the clearest luminosity segregation for late-type Galactic stars among the mid-UV indices. Here, all of the M31 clusters and three of the galaxies have indices significantly stronger than the Galactic library locus. In contrast to Fe I 3000, the clusters form the upper envelope for the galaxies. This is the first index we have discussed where it is reasonably clear that the Galactic library cannot be used to synthesize most of the enhanced cluster or galaxy indices and the anomaly cannot be attributed to UVX contamination affecting the line index itself. On the other hand, it is curious that

the three galaxies with the bluest measures of 2600–3000 (and, by inference, the strongest UVX components) define Mg I 2852 and Blend 3096 relations with 2600–3000 colors that are *more similar* to those of the M31 globular clusters than those defined by the other 4 galaxies.

Figure 5g: Mg Wide index. We calculate this index as it is most likely the index researchers will use to investigate the stellar populations of galaxies at high redshift, when signal-to-noise and bandpass widths are limited. The relationships defined by M31 globular clusters, galaxies and Galactic stars are essentially coincident in this figure.

Comparison of the four Mid-UV line indices measured for Galactic globular clusters by Rose & Deng (1998) to those measured here for elliptical galaxies and M31 globular clusters is shown in Figures 6a-d. Error bars for the HST acquired data are supressed in this figure for clarity. In all four diagrams, the stellar populations of the Galactic globular clusters substantially overlap those of the M31 globular clusters. The offsets between M31 globular clusters and galaxies in the 2609/2660 and Mg II 2800 indices are also seen between the Galactic globular clusters and the galaxies. The Galactic globular clusters define a range in Mg I 2852 vs. 2600–3000 that encompasses both M31 globular clusters and all of the galaxies. Note that two UV indices of M32 (the galaxy lying at 2600–3000 = 1.50) have large differences from those of the Galactic globular cluster 47 Tuc (2600–3000 color, Mg II 2800), to which it is often compared. This reinforces the smaller amplitude distinctions at optical wavelengths discussed by Rose (1994).

### 5. The Near-UV and Blue Indices

Line indices for features in integrated spectra in the near-UV, from 3100Å to 3600Å, just below the Balmer jump, are the current "orphans" of stellar population work. In our perusal of the literature, we have only found three studies that have explored this spectral line region in any depth (Davidge & Clark 1994, Carbon et al. 1982 (and associated references 1982-85), and Boulade, Rose, & Vigroux 1988). Of these, the line indices defined by Davidge & Clark are closest in spirit to the methodology employed here, while the measurements of Carbon et al. and Boulade et al. differ in method and are more specific to their own stellar population measurements.

As with the mid-UV indices, we would like to intercompare the near-UV measurements of the elliptical galaxies and M31 globular clusters with those of Galactic stars. The current stellar data for all but the CN4170 feature are effectively limited to the 16 stars observed by Davidge & Clark. The spectra of stars observed by Boulade et al. were not reduced to fluxes, and hence their measures could not be used here without separate calibrations, which are not available. The CN4170 observations of Davidge & Clark use the Lick (Worthey, et al. 1994) bandpass definition for the "CN1" index. 74 stars with Lick CN1 data were observed by FOBW, making this the only feature with a large stellar sample of both near-UV feature data and mid-UV 2600–3000 colors. The 2600–3000 colors for the Davidge & Clark stars are given in Table 5a, while Table 5b lists the Worthey et al. (1994) CN4170 measures and their 2600-3000 colors from Li et al (1998).

Four of the stars from Davidge & Clark have published 2600–3000 colors in FOBW, and three others have mid-UV colors from other IUE observations (as maintained in our IUE Stellar Library (Li et al. 1998, in preparation.). For the remaining Davidge & Clark stars we estimate their values of 2600–3000 from those given for the average stellar groups in Fanelli et al. (1992) (using the colors given in Table 2 of that paper. We note that owing to a transcription error, the 2600–V and 3000–V colors for the group means listed in Table 7B of Fanelli, et al. 1992 are based on narrow-band rather than intermediate-band fluxes, though the other tabulated quantities are correct.) These 2600–3000 colors should be accurate to 0.10 mag for the non-IUE stars, based on making similar estimates for the Davidge & Clark stars with measured IUE colors.

Figures 7a-f compare the near-UV line indices for galaxies, M31 globular clusters and Galactic stars.

Figure 7a: NH 3360 index. Given previous measurements of strong CN features in the M31 globular clusters and early-type galaxies, measurement of this index is central to the issue of possible nitrogen enhancement in these systems. The NH 3360 values for the Davidge & Clark main sequence stars earlier than K2 V are generally less than 3.00Å. As shown in this figure, the NH 3360 index is obviously far stronger in the M31 globular clusters than in Galactic stars of similar 2600–3000 color. While the formal values of NH 3360 for the galaxies are stronger than for the Galactic stars, the errors on these measures indicate that only the NH 3360 index for NGC 7619 is signficantly above those for the stars, but weaker than those for the M31 globular clusters. These differences must be due to the strength of the NH 3360 index itself and cannot be due to UVX contamination.

Figure 7b: CN 3883. The distribution of M31 globular clusters, galaxies and stars is similar to that found for Bl 3580 and Fe I 3000, rather than as found for NH 3360, in that this index seems to reach a maximum value. Since this index is known to become saturated when the CN molecule becomes too abundant (cf. Langer 1985), it is not surprising that we see little difference between the globular clusters and galaxies here, when we see more of a difference between them in NH 3360.

Figure 7c. Ca HK. This index is mildly enhanced in the more metal-rich globular clusters and the galaxies, being of similar line strength for both kinds of stellar populations at similar 2600–3000 colors. The degree of enhancement is small enough that it is plausible one might be able to fit these measurments with a library of Galactic stars.

Figure 7d. BL 3580. The CN feature at 3580Å lies within this passband (cf. Carbon et al. 1982), but the feature seen is also a blend of many lines due to mostly Fe-peak elements. As such, the relative distribution of values for the M31 globular clusters, galaxies and Galactic stars is very similar to that found for the Fe I 3000 index in the mid-UV (Fig. 5e). The difference here is that most of the galaxies and globular clusters have stronger Bl 3580, relative to the stars, than Fe I 3000. That both galaxies and globular clusters share this difference rules out the UVX component as its main source. The fact that the strength of this blend is not one-to-one with that of CN4170 (cf. Table 3A) for M31 globular clusters suggests that CN is not the principle absorption source for Bl 3580.

Figure 7e. CN 4170. The galaxies and M31 globular clusters define different relationships between 2600–3000 and this CN index than they do with CN 3883 or NH 3360. The globular clusters and three of the galaxies lie on a well-defined locus offset by  $\sim$ 0.15 mag to stronger CN from the galactic stars. Three galaxies have yet stronger CN at a given 2600–3000, but if their colors were corrected for the UVX contribution, it is possible they would lie on an extension of the M31 cluster locus. The CN excesses for the clusters and galaxies were expected on the basis of earlier studies (e.g., Burstein, et al. 1984; Tripicco 1989).

Figure 7f. Break 4000. This break correlates reasonably well with 2600–3000 color, but

shows little difference among M31 globular clusters, galaxies and Galactic stars. As such, this index is as disappointing as the Mg-wide index (Fig. 5g), in that it does not distinguish differences in stellar populations despite differences known in other Mg- and N-related line indices.

Note that, in Figs. 7a-f, the line indices for the three galaxies with blue 2600–3000 colors (NGC 7619, 3608, 5831) show a relationship to those for the redder 2600–3000 galaxies that is partly defined by this color difference. If we had used a color such as B–V for the horizontal axis of these graphs, the line index–color relations would be continuous for the galaxies in these diagrams. However, the general relationship of the M31 globular clusters relative to the galaxies would not be very different.

### 6. Discussion

It has been previously suggested on the basis of high precision optical and infrared photometry or spectra (cf. Frogel, Persson & Cohen 1980, O'Connell 1983, Burstein, et al. 1984, Rose 1985, Burstein 1987, Rose 1994) that the cores of elliptical galaxies, M31 globular clusters, and Galactic globular clusters constitute three distinct types of stellar populations. The mid— and near—UV observations discussed here substantially strengthen this view. The more subtle distinctions which are present in the optical bands are found to be amplified in the mid— and near—UV. However, in the variety of index-color behaviors exhibited, our data also emphasize the complexity of the situation. In this section we discuss these issues.

## 6.1. 2600-3000 Color vs. Optical $Mg_2$

While the 1550–V color employed by Burstein et al. (1988) cleanly separates out very hot stars in a stellar population, the 2600–3000 color depends on the detailed mix of hot and warm stars. It is clear that for globular clusters in our Galaxy and in M31, the dominant contribution of flux to the 2600–3000 spectral region comes from the brightest main sequence stars — typically main sequence turn-off (MSTO) stars. The situation is more complicated for galaxies, as the UVX component can contribute significant flux throughout this wavelength region in the spectra of most giant ellipticals.

As shown in many studies (cf. Frogel, Persson & Cohen 1980; Burstein, et al. 1984) optical and infrared broad-band colors of galaxies, M31 globular clusters and Galactic globular clusters tend to track each other very well. This is also true for some optical absorption line indices, such as Mg<sub>2</sub>, but less so for others (such as the Lick iron line indices Fe 5270 and Fe 5335). In the relationship of UV/optical colors with optical line indices, Burstein et al. (1988) showed that 1550–V color correlates well with Mg<sub>2</sub>, albeit in the opposite sense to optical colors (1500–V becomes bluer with stronger Mg<sub>2</sub>).

Figure 8 shows how  $Mg_2$  is related to 2600–3000 color for galaxies, M31 globular clusters and Galactic globular clusters. To the data in the present paper we have added the 2600–3000 colors for those Galactic globular clusters with  $Mg_2$  measures by Burstein et al. 1984, as well as 2600–3000 colors for representative galaxies from the study of Burstein et al. (1988), combined with the new Trager et al. (1998)  $Mg_2$  measures. We note that the aperture size difference between IUE ( $\sim 8''$  effective diameter; cf. Burstein et al.) and the Lick optical  $Mg_2$  measures ( $\sim 2''$  diameter) did not significantly affect the 1500–V vs.  $Mg_2$  analysis of Burstein et al. Hence, we do not expect using IUE 2600–3000 colors to significantly affect the comparison we make with optical  $Mg_2$  here.

It is evident that the 2600-3000 relation to Mg<sub>2</sub> for these stellar populations is not monotonic. M31 globular clusters and Galactic globular clusters show a general increase in the strength of Mg<sub>2</sub> with redder 2600–3000 color but with the M31 clusters generally having stronger Mg<sub>2</sub> indices than Galactic clusters of similar 2600–3000 color at all colors. One galaxy in this sample, the S0 NGC 5102 (also NGC 205, not shown), has colors similar to the bluest clusters, but this is a well-known star-forming system in which the blue colors result from upper main sequence stars (cf. discussion in Burstein et al. 1988); it is not representative of the other objects in the sample.

The other galaxies appear to fall into two loosely-defined groups. One group of 4 (NGC 4382, NGC 5018, NGC 3605 and M32) is coincident with the reddest and most metal-rich clusters. A larger group has significantly higher Mg<sub>2</sub> showing relatively small scatter in the index but large 2600–3000 scatter. This is similar to what is seen when Mg<sub>2</sub> is plotted versus the 1550–V color of Burstein et al. (1988), in that the line index varies little while the 1550–V color varies over nearly 2 magnitudes. This strongly suggests that the UVX component that gives rise to the 1550–V range in color among ellipticals is also important in determining the 2600–3000 range in color.

We can estimate how much UVX contamination would be necessary to produce the blueward scatter of the strong-lined objects. An extrapolation of the relatively shallow slope of the line-color correlation in Figure 8 for the clusters and the redder galaxy group predicts a 2600–3000 color near 2.0 for objects with Mg<sub>2</sub> values comparable to those in the

strong-lined group. Adopting a 2600–3000 color for the UVX objects of  $\sim -0.5$ , we find that the UVX would have to contribute over 65% of the light at 2600 Å in order to shift the strong-lined objects to 2600–3000 colors of < 1.0. This is reasonably consistent with our estimate (§4) of over 50% contamination of the UVX component of the 2600 bandpass when the UVX component is strong.

Obviously, a larger sample of UV data is needed to explore this correlation further. On the basis of the present sample alone, it appears that the galaxies themselves may fall into several discrete groups. Galaxies in several of the other line index-color diagrams (notably BL 3096, Fig. 5f) also have a clump-like distribution. Hints of similar discreteness in the comparison of fluxes at 1500Å, 2500Å, and the V-band with Mg<sub>2</sub> were pointed out by Dorman et al. (1995). This would imply that metallicity, as measured by Mg<sub>2</sub>, is not the only driver of the amplitude of the UVX component. A similar conclusion is reached by Ohl et al. (1998) on the basis of UV color and line strength gradients inside ellipticals.

As a separate issue, it is not clear why the M31 globular clusters should have stronger Mg<sub>2</sub> indices than Galactic globular clusters at a given 2600–3000 color. As we are comparing HST FOS data with IUE data, it is possible that systematic errors could play a role. While reliable errors for the IUE cluster data are difficult to determine, it is hard to see how the errors could be as large as the 0.3–0.5 magnitude 2600–3000 color difference we do see.

#### 6.2. Nitrogen-Dependent Indices

Burstein et al. (1981; 1984) first pointed out that CN line indices were significantly stronger in M31 globular clusters than Galactic globular clusters of the same B–V color. This discovery was later confirmed by Tripicco (1989). As shown in Figure 7, the three near-UV line indices involving nitrogen: CN 4170, CN 3883 and NH 3360 show marked enhancements relative to Galactic stars for both galaxies and M31 globular clusters. Whereas interpreting the strength of CN in terms of nitrogen abundance is complicated by questions of carbon abundances and the mixture of main sequence and giant-branch light (molecular abundances are very sensitive to surface gravity), NH is notably cleaner because only the one metal is involved and the light at 3300Å is dominated by main sequence stars.

The fact that the M31 globular clusters are over-enhanced the *most* in NH 3360 relative to Galactic stars is a clear indication that the M31 globular cluster stars are overabundant in nitrogen. How overabundant? Look at the spectrum of MIV, the globular cluster in M31 with similar colors and optical line strengths as M92 (NGC 6341), one of

the most metal-weak globular clusters in our own Galaxy. Carbon et al. (1982) studied the temperature, gravity and abundance dependence of NH 3360 in the spectra of the giant stars of M92. They show that, in this low abundance range, the NH 3360 feature is little dependent on gravity, but primarily dependent on temperature and abundance. In particular, NH 3360 all but disappears in stars with effective temperatures hotter than 5500 K. The MSTO stars in M92 are hotter than this temperature, and it is these stars that contribute the bulk of the flux at 3360Å in this metal-poor cluster (cf. discussion by Rose 1994), and, by association, in MIV.

Moreover, it seems that the NH feature reaches something approaching a "saturation level" in the more metal-rich M31 globular clusters, reaching a near-constant value of ~ 7.5Å. Such an effect is also seen in the CN 3883 index where it is known to be a saturation effect (Langer 1985). The strong enhancement of both NH 3360 and CN 4170 in M31 globular clusters relative to Galactic stars means that the enhancement of CN 4170 in M31 globular clusters relative to Galactic globular clusters found by Burstein et al. (1984) is also due to a nitrogen overenhancement. Significantly, the NH 3360 index for these galaxies is also enhanced relative to Galactic stars, but is generally lower than for the M31 globular clusters. (Interestingly, Boulade et al. (1993) found NH3360 strength in M32 to be reasonably fit with a Galactic stellar population.) Thus, we are left with another unanswered question: Why are many old stellar populations outside our Galaxy enhanced in nitrogen abundance relative to the disk and halo stars near us and to the stars in Galactic globular clusters?

## 6.3. Mg-related Indices

It has already been shown by Gonzalez (1993) and Trager (1996) that the optical Mg<sub>2</sub> index is overly strong in the stellar populations of early-type galaxies, compared to optical Fe-based indices and stellar population models made from Galactic stars. The M31 clusters also appear to be significantly stronger in Mg<sub>2</sub> than Galactic clusters, compared to their 2600–3000 colors, though both are significantly weaker in Mg<sub>2</sub> than most galaxies (Fig. 8; see, however, the Mg<sub>2</sub> - B–V relations for these same clusters in Burstein, et al. 1984).

Paradoxically, these relationships fail to hold for the UV Mg I and Mg II indices, relative to the 2600–3000 color. Behavior of the Mg I 2852 index (Fig. 6d) for the two sets of clusters may parallel that of Mg<sub>2</sub> in Fig. 8, but the two cluster samples appear to overlap in the Mg II 2800 index (Fig. 6c). Furthermore, the galaxies are no stronger in Mg I 2852 than the clusters and are actually significantly weaker in Mg II.

Given the optical-band Mg<sub>2</sub> results, the galaxies are clearly not underabundant in magnesium itself. There are at least three possible effects which may operate to produce the UV Mg anomalies in galaxies. First is UVX contamination, which could dilute the Mg II strengths, though as noted in Sec. 4.2 this does not seem capable of explaining the entire Mg II anomaly. Second is the fact that the Mg II index actually declines in more metal-rich stars, apparently owing to large line blanketing in the sidebands (FOBW, Fanelli, et al. 1992). The third possibile effect is Mg II line reversal by chromospheric emission. This is clearly detectable in individual stars (Smith et al. 1991). However it is only present in stars younger than 1–2 Gyr (according to conventional Ca II chromospheric emission dating scales). While there is good evidence for the presence of intermediate age populations in the range 4–8 Gyr in some of our sample elliptical galaxies (Gonzalez 1993, Trager 1996), components with ages in the 1–2 Gyr range are usually excludable because of their gross effect on the continuum energy distribution. However, it may be that the chromospheric and galaxy spectral age scales are not yet mutually consistent.

As a separate consideration, it is clear from the distinct behavior of the elliptical galaxies and star clusters in the Mg indices that a metal-poor (cluster-like) stellar population is *not* likely to be dominant at far–UV wavelengths in the galaxies, as had been claimed by Park & Lee (1997), among others.

# 6.4. The Other UV Indices

### 6.4.1. Breaks 2609/2660 and 2828/2921

The 2609/2660 index is the most affected by flux from the far-UV strong stellar population in galaxies among all of the indices measured in this paper. The galaxies as a group are offset from the globular clusters as a group by  $\approx 0.3$  mag. As we know the ellipticals have a strong UVX component in their UV spectra that is missing in the globular clusters, it is likely that the index offset is explained mainly by UVX contamination. Rose & Deng (1998) also show that the offset between 47 Tuc and M32 (the reddest galaxy in Fig. 6a) can be explained by the weak UVX component (Burstein, et al. 1988) in M32 that is not in 47 Tuc.

The 2828/2921 index shows reasonable agreement among all of the globular clusters and galaxies, with perhaps an intrinsic spread of about 0.1 mag. Given this general agreement, it is likely that this index can be fit in all of the stellar populations with the

normal Galactic library. UVX contamination is evidently considerably less at 2900Å than at 2600Å.

## 6.4.2. Fe I 3000 and Bl 3580

Both of these indices are dominated by a series of strong Fe I lines, although the BL 3580 index is also somewhat affected by CN. The apparent excess line strengths in Figs. 5e and 7d may be explainable by compositeness effects — i.e., the combination of cool and warm stars from the normal Galactic library, together with the presence of hot UVX stars in some of the galaxies. Detailed modeling would be required to confirm that, however.

## 6.4.3. Blend 3096

This is the first time this feature has been reliably measured in external stellar populations. Examination of the solar spectrum (Moore et al. 1966) shows the strongest lines in the central bandpass of 3086–3106Å are due to Al I (at 3092.7Å) and Mg I (at 3096.9Å), combined with weaker lines of Fe I, Ti II, Ni I and OH. To our surprise, this index is so strong in the strongest-lined globular clusters and in NGCs 3608, 5831 and 7619 that it appears no combination of Galactic stars can fit it.

A close up examination of the observed spectra of the M31 globular clusters (where internal velocity dispersion does not erase fine detail) shows this feature to be double-peaked in absorption, with the separation of the two peaks of about  $6\text{\AA}$ . One peak is around  $3092\text{\AA}$ , and can be reasonably associated with the Al I line. The other peak is around  $3098\text{\AA}$ , and is likely a combination of the strong Mg I feature plus the relatively strong Fe I lines between  $3099-3101\text{\AA}$ .

The strength of this feature in the M31 globular cluster spectra and in a subset of the galaxies is such that it is not just due to the known Mg I enhancement, but also must involve an enhancement in aluminum as well. This is the first time, to our knowledge, that an enhancement in Al has been found in extragalactic stellar systems. These three low-resolution line indices measure some of the most prominent features in the integrated spectra of old stellar systems: strong breaks in the spectra around the Ca H&K features near 4000Å and near the Mg I 2852 and Mg II 2800 features. These are the line strengths workers have used to try to measure evolution in stellar populations at high redshift (e.g. Windhorst et al. 1994). It is therefore disappointing that, whereas we can identify three separate stellar populations among M31 globular clusters, elliptical galaxies and Galactic stars/globular clusters in other line indices, these three indices are insensitive to these distinctions. As Rose (1994) and others have pointed out, lower resolution measures of old stellar populations can suggest a deceptive uniformity.

## 6.5. The M31 Globular Cluster HST Color-Mag Diagrams

Fusi-Pecci et al. (1996) have published color-magnitude diagrams (V vs. B–V and I vs. V–I) for the four M31 globular clusters in our study. While the metallicities estimated from the giant branches for MIV, MII and K280 are reasonably in agreement with the metalliticies we would estimate from our FOS observations, K58 stands out as a notable exception. Whereas Fusi-Pecci et al. would have K58 be only slightly more metal-rich than MII, both the Brodie & Huchra measurement of its optical Mg<sub>2</sub> index, as well as our FOS spectra, indicate this globular cluster likely has somewhat above solar metallicity. Some confusion in ranking the clusters via the CM diagrams might be the result of using V–I for some and B–V for others (e.g., K58). A V–I diagram for K58 would be interesting, as it is possibly metal-rich enough to have its I band flux saturated via an extreme nitrogen overabundance, much like Frogel et al. result for the bulge of our Galaxy (Frogel & Whitford 1987)? Clearly accurate integrated spectra of these, and other M31 globular clusters into the near-infrared would be of interest.

#### 7. Conclusions

The same two elemental "suspects" come up time and again when intrinsic differences among stellar populations are discussed: nitrogen and magnesium. To this list, we now can perhaps add aluminum based on the behavior of the Bl 3096 index. One important contribution of our observations is that variations in nitrogen abundance have been cleanly identified. It is clear from the enhanced NH 3360 features, especially in the M31 globular

clusters, that as a group these four clusters have stars that are substantially enhanced in nitrogen compared to Galactic stars. Based on the models of Carbon et al., it is possible that the overabundance reaches factors of 10-50 in the M31 clusters. Nitrogen abundance estimates based on the CN indices longward of 3800Å are made ambiguous because of the involvement of carbon and because the indices are more sensitive to the mixture of giant and dwarf light. The value of the NH 3360 feature in old stellar population spectra is that it isolates nitrogen and that dwarf light dominates at this wavelength.

The inferred large overabundance of nitrogen in the M31 globular clusters does not conflict with the known agreement of broad-band colors between M31 and Galactic globular clusters. Nor does it conflict with the fact that the HST-derived color-mag diagrams of these same globular clusters (cf. Fusi-Pecci et al. 1996) yield giant branch slopes generally consistent with their derived broad-band colors. As Carbon et al. show, stars with very different atmospheric abundances of nitrogen exist side-by-side in the color-mag diagram of M92. Moreover, theoretical studies by VandenBerg (e.g. vandenBerg & Stetson 1991) show that increasing only the oxygen abundance does not change the structure of the HR diagram, but rather makes the cluster look older than it really is. As the same is likely to be true for nitrogen, HR diagrams alone will not divulge nitrogen abundance differences among different stellar populations.

The combination of enhancements in N, Mg and perhaps Al are unusual, as each is thought to come from different kinds of stars: N from low mass stars; Mg direct from C—and O—burning; Al from a combination of C—and Ne—burning, but also tied directly to O abundance. Laird (1985) and Boulade et al. (1988) both found low metallicity stars with large (5–50) overabundances in nitrogen. Norris & Smith (1983) point to a possible connection between overenhancements of N, Na and Al in Galactic globular cluster giant stars. It would obviously be useful to attempt to measure Na abundances in elliptical galaxies from prominent features like the Na I D lines at high enough spectral resolution that contamination from interstellar absorption can be eliminated.

Our observations have also emphasized the importance of the effects of the hot UVX component at wavelengths as long as 3000Å. This is a potentially serious complication for the age-dating of high redshift galaxies based on restframe mid–UV spectra. At present, we do not understand the UVX component well enough to predict its strength from first principles; only direct observations of the restframe far–UV spectra suffice to determine its amplitude. This is particularly true if it is not simply related to a single parameter like metallicity, as suggested by the apparent discreteness of the galaxy distribution in some of our correlations.

Other implications of these results for the study of stellar populations of early-type

galaxies, both nearby and at high redshift, will be discussed further in Ponder et al. (1998).

# 8. Acknowledgements

DB, CCW, RWO, JAF and JAR all wish to thank and acknowledge the support of NASA Grants GO-2298-87A and GO-6585-95A for this research, and the referee for helpful comments. DB wishes to thank the hospitality of the Space Telescope Science Institute during his visits and the assistance of Mr. Yong Li. CCW specifically wishes to acknowledge that this project is supported by the research contract GO-06585.04-95A awarded to the Computer Sciences Corporation by Space Telescope Science Institute which is operated by the Association of Universities for Research in Astronomy, Inc., for NASA under contract NAS5-26555. RWO was also supported in part by NASA grant NAG5-6403 to the University of Virginia.

#### REFERENCES

- Battistini, P., Bonoli, F., Braccesi, A., Fusi-Pecci, F., Malagnini, M.L., & Marano, B. 1980, A&AS, 42, 357
- Battistini, P., Bonoli, F., Braccesi, A., Federici, L., Fusi-Pecci, F., Marano, B. & Borngen, F. 1987, A&AS, 67, 447
- Baum, S. 1993, ed. FOS Data Products Guide, ST ScI. (DPG)
- Bertola, F., Burstein, D., & Buson, L.M. 1993, ApJ, 402, 573
- Boulade, O., Rose, J.A., & Vigroux, L. 1988, AJ, 96, 1319
- Brodie, J. P. and Huchra, J. P. 1990, ApJ, 362, 503
- Brown, T.M., Ferguson, H.C., & Davidsen, A.F. 1995, ApJ, 454, 19
- Burstein, D., Faber, S.M., Gaskell, C.M. & Krumm, N., 1981, in IAU Colloq. 68, A.G.D. Phillips, ed., p. 441
- Burstein, D., Faber, S. M., Gaskell, C. M., & Krumm, N. 1984, ApJ, 287, 586
- Burstein, D. 1987, in Nearly Normal Galaxies: From the Planck Time to the Present ed. S.M. Faber, (Springer-Verlag), p 47

Burstein, D., Bertola, F., Buson, L.M., Faber, S.M., & Lauer, T.R. 1988, ApJ, 328, 440

Burstein, D. & Heiles, C. 1984, ApJS, 54, 33

Buson, L.M., Bertola, F. & Burstein, D. 1990, in Windows on Galaxies, eds. G. Fabbiano, J.S. Gallagher & A. Renzini, (Kluwer: Boston), p 51

Cacciari, C., Cassatella, A., Bianchi, L., Fusi-Pecci, F. & Kron, R.G. 1982, ApJ, 261, 77

Carbon, D.F., Romanishin, W., Langer, G.E., Butler, D., Kemper, E. Trefzger, F., Kraft, R.P. & Suntzekff, N.B. ApJS, 49, 207

Cardelli, J. A., Clayton, G. C., & Mathis, J. S. 1989, ApJ, 345, 245

Charlot, S., Worthey, G. & Bressan, A. 1996, ApJ, 457, 625

Christensen, C.G. 1972, Ph.D. Thesis, Cal Inst Tech

Cowley, A.P. & Burstein, D. 1988, AJ, 95, 1071

Crotts, A.P.S, Kron, R.G., Cacciari, C., & Fusi-Pecci, F. 1990, AJ, 100, 141

Davidge, T. J., and Clark, C. C. 1994, AJ, 107, 946

de Vaucouleurs, G., de Vaucouleurs, A., Corwin, H.G., Jr., Buta, R.J., Paturel, G. & Fouqué 1991, Third Reference Catalog of Bright Galaxies, (New York: Springer-Verlag) (RC3)

Dorman, B. O'Connell, R.W. & Rood, R.T. 1995, ApJ, 442, 105

Faber, S. M. 1973, ApJ, 179, 731

Faber, S. M., Friel, E. D., Burstein, D., & Gaskell, C. M. 1985, ApJS, 57, 711

Faber, S.M., Wegner, G., Burstein, D., Davies, R.L., Dressler, A., Lynden-Bell, D. & Terlevich, R. 1989, ApJS, 69, 763

Fanelli, M. N., O'Connell, R.W., Burstein, D., & Wu, C.-C. 1990, ApJ, 364, 272 (FOBW)

Fanelli, M.N., O'Connell, R.W., Burstein, D., & Wu, C.-C. 1992, ApJS, 82, 197

Frogel, J.A., Persson, S.E., Cohen, J.G. 1980, ApJ, 240, 785

Frogel, J.A. & Whitford, A.E. 1987, ApJ, 320, 199

Fusi-Pecci, F., Buonanno, R., Cacciari, C., Corsi, C.E., Djorgovski, S.G., Federici, L., Ferraro, F.R., Parmeggiani, G., Rich, R.M. 1996, AJ, 112, 1461

Gonzalez, J. J. 1993, PhD Thesis, U.C. Santa Cruz

Greggio, L. & Renzini, A. 1990, ApJ, 364, 35

Harris, W. 1997, WEB page on Galactic Globular Clusters: www.physics.mcmaster.ca/Globular.html

Hayes, D. S. & Latham, D. W. 1975, ApJ, 197, 593

Huchra, J.P., Brodie, J.P., & Kent, S.M. 1991, ApJ, 370, 495

Langer, G.E. 1985, PASP, 97, 382

Li, Y., Burstein, D., Wu, C.-C., O'Connell, R.W., Bohlin, R., Stryker, L.L. 1998, in preparation

Laird, J. 1985, ApJ, 289, 556

Mayall, N. & Eggen, O. 1953, PASP, 65, 24

Moore, C.F, Minnaert, M.G.J., & Houtgast, J. 1966, "The Solar Spectrum 2935 to 8770 Angstroms," NBS Monograph 61

Norris, J. & Smith, G.H. 1983, ApJ, 272, 635

O'Connell, R.W. 1973, AJ, 78, 1074

O'Connell, R.W. 1980, ApJ, 236, 430

O'Connell, R.W. 1983, in Highlights of Astronomy, ed. R. West (Reidel: Dordrecht), 147

O'Donnell, J.E. 1994, ApJ, 422, 1580

Ohl, R.G. et al. 1998, in preparation

Park, J.-H. & Lee, Y.-W. 1997, ApJ, 476, 28

Peterson, C.J. 1993, in Structure and Dynamics of Globular Clusters, ASP Vol 50, eds. S.G. Djorgovski & G. Meylan (ASP: San Francisco), p. 337

Ponder, J., Burstein, D. Frogel, J.A., O'Connell, R.W., Rose, J., Tripicco, M., Wu, C.-C. 1998, ApJ,l, in preparation

Rose, J.A. 1985, AJ, 90, 1927

Rose, J.A. 1994, AJ, 107, 206

Rose, J.A. & Deng, S. 1998, AJ, submitted

Sargent, W.L.W., Kowal, C.T., Hartwick, F.D.A., & van den Bergh, S. 1977, AJ, 82, 947

Seaton, M. 1979, MNRAS, 187, 73p

Smith, G.H., Burstein, D., Fanelli, M.N., O'Connell, R.W. & Wu, C.-C. 1991, AJ101, 655

Tantalo, R., Chiosi, C., Bressan, A., & Fagatto, F. 1996, A&A, 311, 361

Trager, S.C. 1996, Ph.D. Thesis, University of California, Santa Cruz

Trager, S.C., Worthey, G., Faber, S.M., Burstein, D. & Gonzalez, J.J. 1998, ApJS, in press

Tripicco, M. J. 1989, AJ, 97, 735

van den Bergh, S. 1969, ApJS, 19, 145

vandenBerg, D.A. & Stetson, P.B. 1991, AJ, 102, 1043

Wilson, O.C. 1963, ApJ, 138, 832

Windhorst, R. A., Pascarelle, S. M., Keel, W. C., Bertola, B., McCarthy, P. J., O'Connell, R. W., Renzini, A., & Spinrad, H. 1994, in Frontiers of Space and Ground-Based Astronomy, eds. E. W. Wamsteker, M. S. Longair, & Y. Kondo (Dordrecht: Kluwer), p 663

Worthey, G., Faber, S. M., Gonzalez, J. J., & Burstein, D. 1994 ApJS, 94, 687

Worthey, G. 1992, Ph.D. thesis, University of California, Santa Cruz

Yi, S., Demarque, P. & Oemler, A., Jr. 1997, ApJ, 486, 201

This preprint was prepared with the AAS IATEX macros v3.0.

# A. Appendix A. Target Acquisition

Precise centers of diffuse objects such as galaxies and globular clusters are difficult to determine from ground-based data. As such, the FOS must employ a search procedure to place the center of these objects in the science aperture. In acquiring each object, the telescope scans an area of sky around the input coordinates. The target acquisitions use various apertures and scanning patterns to determine the position with the greatest flux for that aperature.

The first  $(3\times1)$  scan (4.3'') aperture and sweeps out a rectangle of six by two integration positions. The third  $(3\times3)$  scan takes an s-shaped pattern of integrations with the 0.5'' aperture. The fourth scan  $(4\times4)$  also sweeps out an s-shaped pattern with a 0.3'' aperture. Integration times per position in these scans are necessarily short (5s-60s) to keep the acquisition times within reasons (even then, they typically take 2-3 orbits). The fact that the M31 globular clusters have small apparent effective radii, combined with relatively accurate initial positions, allowed us to point to these objects effectively with only the first three acquisition scans. In the case of the elliptical galaxies, the uncertainty of the positions of the cores of the galaxies prompted us to use all four sets of acquisition scans.

As the FOS could saturate on these aquisition scans, a reasonable estimate of expected flux was required to maximize the set-up signal while not getting too much flux. As we knew best the UV fluxes of our sources from their IUE observations, it was decided to use the G270H grating as part of the acquisition procedure. This had the added benefit of being able to see in each acquisition scan the spectrum of the position sampled. To verify the accuracy of the target acquisition, we reduced each of these scanned spectra, and plotted them using the celestial positions from their header files. An example of one 3×3 scan of one M31 globular cluster (K58) is shown in Figure 9 as an example. The S/N seen in these aquisition spectra are poor, in keeping with the short exposure times. Due to the changing sizes of the scan apertures, the positions of greatest flux in each successive set of spectra can shift within one scan position, owing to the quantized scan search.

For each scanned spectrum, we determined its 2600–3000 color for both intercomparison and comparison to the color we obtained with our program spectrum. By comparing the color for each scanned spectrum, the determined centers, and the observed spectrum, we can determine the reliability of each acquisition. The colors determined from the science observations of K280, MII, and MIV agree with the centers determined by the 3×3 scan. As seen in Figure 10, the agreement is worse for the globular cluster K58, which has the lowest UV surface brightness among the four M31 clusters. Even so, the aquisition colors are

within nominal expected limits of the actual observed 2600-3000 color as given in Table 3A ( $2\sigma$  for this many observations and the poor S/N of the acquistion spectra).

For the elliptical galaxies, obtained in Cycles 4 and 6, the FOS aquisition procedure used all four sets of scans to acquire diffuse objects. In every case, we confirm accurate registration of the FOS observation aperture with the source of maximum UV flux in the galaxies.

Fig. 1a.— The de-redshifted, extinction-corrected FOS G270H spectra of the four M31 globular clusters. The spectral range is 2250 Å to 3270 Å. The identification of the mid-UV absorption and spectral break features used in this paper are indicated on the spectrum of MII.

Fig. 1b.— Same as Figure 1a, but for the FOS G400H grating — a spectral range of 3200 Å to 4780 Å. The identification of near-UV line absorption and spectral break features are indicated on the spectrum of MII.

Fig. 2a.— The de-redshifted, extinction-corrected FOS G270H spectra of the six elliptical galaxies. The spectral range is 2250 Å to 3270 Å.

Fig. 2b.— Same as Figure 2a, but for the FOS G400H grating — a spectral range of 3200 Å to 4780 Å.

Fig. 3.— These figures show the full FOS spectra of the M31 globular clusters given on a logarithmic flux scale from 2250 Åto 4780 Å. The FOS G270H spectrum overlaps that of the G400H spectrum by 70 Å. As can be seen, the absolute flux levels of the two gratings agree to within 5%.

Fig. 4a.— The full FOS spectra of three of the elliptical galaxies, NGC 3605, NGC 3608 and NGC 5018, given on a logarithmic flux scale from 2250 Åto 4780 Å. The agreement in overall flux level between the G270H and G400H spectra is well within 5%, and is better than for the spectra of the M31 globular clusters.

Fig. 4b.— The full FOS spectra of three of the elliptical galaxies, NGC 5831, NGC 6127 and NGC 7619, given on a logarithmic flux scale from 2250 Å to 4780 Å. Also plotted is the IUE merged LWP spectrum for M32, as taken from Buson et al. (1990).

Fig. 5a,b.— This figure is in 7 parts (a–g), showing how the mid-UV line indices and spectral breaks derived from the FOS spectra of the four M31 globular clusters, the FOS spectra of the six elliptical galaxies, and the IUE spectrum of M32 compare to those derived for Galactic stars from IUE LWP spectra by FOBW. In each case, the X-axis is the mid-UV color 2600–3000 (in magnitudes). All line indices and spectral breaks are also measured in magnitudes. In each figure the small, subdued symbols indicate the stars taken from FOBW. Only dwarfs (open squares), subgiants (open triangles) and giants (open diamonds) are plotted. The large closed symbols are the data for the M31 globular clusters; K58 (square), K280 (triangle), MII (inverted triangle), and MIV (diamond). The large open symbols denote the galaxies: M32 (circle), NGC 3605 (inverted triangle), NGC 3608 (asterisk), NGC 5018 (diamond), NGC 5831 (triangle), NGC 6127 (square), NGC 7619 (cross). Only the 2600–3000 error bar is given for NGC 5018; for all other HST-observed objects the 2600–3000 error is smaller than the plot symbol size. (a) The 2609/2660 spectral break. (b). The 2828/2921 spectral break.

Fig. 5c,d.— Same symbols as for Figures 5a,b. c) The Mg II 2800 line index. d) The Mg I 2852 line index.

Fig. 5e,f.— Same symbols as for Figures 5a,b. e) Fe I 3000 line index. f) The BL 3096 line index, mostly measuring Al, Mg and Fe.

Fig. 5g.— Same symbols as for Figures 5a,b. g) The Mg Wide line index, basically measuring the break in the continuum produced by the Mg II 2800 and Mg I 2852 lines.

Fig. 6.— This figure redisplays Figures 5a–d, but this time adding the Galactic globular clusters from Rose & Deng (1998) and not plotting the data for Galactic stars. Error bars are supressed for clarity. In this way, the comparisons among the Galactic globular clusters, M31 globular clusters and elliptical galaxies are more clearly seen. Data for Galactic globular clusters are plotted as small closed squares, for M31 globular clusters as large open circles, and for galaxies as large open triangles. (a) 2609/2660 spectral break. (b) 2828/2921 spectral break. (c) Mg II 2800. (d) Mg I 2852.

Fig. 7.— The near-UV absorption line indices and the 4000 Å spectral break taken from the G400H FOS spectra. Small symbols here represent the data for Galactic stars taken from the study of Davidge & Clark (1994) for all six indices, supplemented by data taken from the stars given in Worthey et al. (1994) for the CN4170 index. The large symbols represent the four M31 globular clusters and the six galaxies observed with the FOS G400H grating, using the same coding as in Figures 5a-g. Errors in 2600–3000 are smaller than symbol size for the HST data in these figures, and are not shown. a) NH 3360; b) CN 3883; c) Ca HK; d) Bl 3580; e) CN 4170; and f) 4000 Å spectral break.

Fig. 8.— The optical line index, Mg<sub>2</sub> plotted versus the 2600–3000 color for four sets of data: M31 globular clusters (closed circles); Galactic globular clusters (open squares); the six elliptical galaxies studied here (closed triangles) and a representative set of early-type galaxies taken from the IUE galaxy study of Burstein et al. (1988) (open triangles). Note the range of Mg<sub>2</sub> at a fixed 2600–3000 color, indicating the relationships of optical colors and line indices with 2600–3000 color are complicated.

Fig. 9.— The three by three G270H spectral scans of the M31 globular cluster K58 taken during target acquisition with the FOS. This is by far the worst case among the 10 FOS object acquisitions done for this project. The box size for each spectrum does not represent the size of the aperture (for  $3 \times 3$  scanning, aperature size is 0.5''). The small circled x in Box 7 indicates that this was the position that the acquisition process picked for maximium flux. Comparing to Box 6, we see indication that there may be a misalignment. But, because the aperture sizes are in general larger than the amount by which the telescope has been shifted, the position of greatest flux may not appear to be the optimium position.

Fig. 10.— How well did the FOS aquisition work? This figure plots the 2600–3000 colors derived from each acquistion G270H spectrum. The symbols used represent the colors obtained from the individual scans (small symbols: open square for the initial  $3\times1$  scans with the 4.3" full aperture; open diamonds for second  $2\times6$  scans with the 1.0" aperture; open triangles for the third and final  $3\times3$  scans with the 0.5" circular aperture). The color for the scan center selected by the aquisition process for each scan is denoted by a large symbol (cross for  $3\times1$  center; plus sign for  $2\times6$  center; circle for  $3\times3$  center). The 2600-3000 color obtained from our program observation is indicated by a large square. Note that for all but K58, the 2600-3000 color from the  $3\times3$  center and that from the program observation are very similar. For K58 the difference is greater, owing to the lower S/N spectra for this cluster.